

SAND88-2267
Unlimited Release
September 1988

STRATEGIC PETROLEUM RESERVE (SPR)
ADDITIONAL GEOLOGICAL SITE CHARACTERIZATION STUDIES
BIG HILL SALT DOME, TEXAS

Thomas R. Magorian
Consultant
Amherst, New York

James T. Neal
SPR Geotechnical Division 6257
Sandia National Laboratories
Albuquerque, New Mexico 87185

ABSTRACT

The salt mass at Big Hill dome, Texas, has been characterized using information from 28 wells that were drilled in preparation for solution mining of fourteen new 11.5 MMBBL caverns for the Strategic Petroleum Reserve. Beneath an exceptionally thick caprock (-1350 ft), the salt is very pure, with an average anhydrite content of about 1.7%, and only minor shale and sylvite along the southern tier of caverns. Anhydrite distribution between holes is correlative on the density logs, revealing two distinct spines in the salt mass. These are separated by a north-northeast-trending shear zone that is structurally aligned with the High Island- Spindletop salt ridge and parallels the Hackberry Embayment, a major Gulf Coast feature. The shear zone appears to displace the caprock down to the east by as much as 100 ft. The shear zone may not transect any caverns, but this cannot be ruled out at present. The anhydrite layering on the southern edge may enhance the cavern/dome-edge separation, but minor sylvite may also produce irregularities. Additional cavern space along the western and southern boundaries cannot be ruled out until further exploration is completed. Other space is available to the north, and probably has better potential for expansion. The results further substantiate the conclusions of the original geological site characterization report (SAND81-1045) that the site is geologically superior for SPR cavern development. No new information has detracted from this position, but a continuing surveillance effort is advocated to monitor subsidence and other cavern-induced effects.

TABLE OF CONTENTS

	Page
1.0 Introduction	5
2.0 Geology of the Salt Dome	6
2.1 Geological Interpretation.....	6
2.2 Evaporite Mineralogy	6
2.2.1. Halite	6
2.2.2. Insolubles	9
2.2.3. Other Constituents.....	1 3
2.3 Interior Structure from Well Logs/Core Validation.....	1 3
2.3.1. Spines.....	14
2.3.2. Shear Zone.....	15
2.3.3. Salt Ridge.....	15
2.3.4. Dome-Related Faulting.....	1 6
2.4 Caprock Geology and Hydrology.....	1 6
2.4.1. Caprock Faulting.....	1 7
2.5 Cross Sections Through Caverns.....	1 7
3.0 Potential Expansion Areas for Additional Storage	2 4
3.1 Cavern Layout.....	2 4
3.2 Exploratory Measures for Expansion of Caverns.....	2 4
4.0 Geotechnical Considerations.....	2 6
4.1 Cavern Leaching.....	2 6
4.2 Natural Hazards: Subsidence Effects.....	2 6
4.3 Lessons Learned: Drilling and Logging.....	2 6
4.3.1. Lost Circulation.....	2 6
4.3.2. Hydrogen Sulfide.....	2 7
4.3.3. Well Logging and Coring.....	2 7
5.0 Summary and Conclusions.....	2 8
6.0 References.....	7 0
Appendix A. Summary of Background Geological Information.....	3 0
Appendix B. Anhydrite Correlations.....	3 4

LIST OF TABLES

1.	Big Hill SPR Site Tertiary Geologic Units.....	2 0
B-1	Cavern101.....	36
B-1	Cavern 202	37
B-1	Cavern103.....	38
B-1	Cavern104.....	39
B-1	Cavern105.....	40
B-1	Cavern106.....	41
B-1	Cavern 106 (continued).....	4 2
B-1	Cavern107.....	43
B-1	Cavern108.....	44
B-1	Cavern109.....	45
B-1	Cavern 110	46
B-1	Cavern 110 (continued).....	4 7
B-1	Cavern 111.....	48
B-1	Cavern 111 (continued).....	49
B-1	Cavern 112	50
B-1	Cavern113.....	51
B-1	Cavern114.....	52
B-2	Anhydrite.....	69

LIST OF FIGURES

1.	Big Hill Salt Dome Structure Map - Salt	7
2.	Core taken from 106A at -3507 ft showing single-crystal salt of exceptional purity	8
3.	Photo of core taken from 106B, -5475-80 ft, showing typical banded anhydrite	10
4.	Photo of core taken from 106A at -2527 ft showing broken chunks of anhydrite	11
5.	Photo of core taken in 110B at -4510 ft showing massive halite (left) and crystalline anhydrite (scale in inches and tenths of ft)	12
6.	Big Hill Salt Dome Structure Map - Caprock	
	West-East cross section No. 1, Big Hill Salt Dome; T. R. Magorian, April, 1988	19
8.	West-East cross section No. 2, Big Hill Salt Dome; T. R. Magorian, April, 1988	21
9.	West-East cross section No. 3, Big Hill Salt Dome; T. R. Magorian, April, 1988	22
10.	Northwest-Southeast cross section, Big Hill Salt Dome; T. R. Magorian, April, 1988	23
B-1	Big Hill salt dome anhydrite correlations neutron density log cavern 111 well A	53
B-1	Big Hill salt dome anhydrite correlation neutron density log' cavern 111 well B	54
B-2	Big Hill salt dome anhydrite correlations SPR Cavern 101	55
B-2	Big Hill salt dome anhydrite correlations SPR Cavern 102	56
B-2	Big Hill salt dome anhydrite correlations SPR Cavern 103	57
B-2	Big Hill salt dome anhydrite correlations SPR Cavern 104	58
B-2	Big Hill salt dome anhydrite correlations SPR Cavern 105	59
B-2	Big Hill salt dome anhydrite correlations SPR Cavern 106	60
B-2	Big Hill salt dome anhydrite correlations SPR Cavern 107	61
B-2	Big Hill salt dome anhydrite correlations SPR Cavern 108	62
B-2	Big Hill salt dome anhydrite correlations SPR Cavern log	63
B-2	Big Hill salt dome anhydrite correlations SPR Cavern 110	64
B-2	Big Hill salt dome anhydrite correlations SPR Cavern 111	65
B-2	Big Hill salt dome anhydrite correlations SPR Cavern 112	66
B-2	Big Hill salt dome anhydrite correlations SPR Cavern 113	67
B-2	Big Hill salt dome anhydrite correlations SPR Cavern 114	68

1.0 INTRODUCTION

Big Hill Salt Dome characterization studies were conducted in 1980-81 and provided input to establish the geotechnical suitability of emplacing oil in 14 solution cavities within the dome. The use of this dome combined with Weeks Island, Bayou Choctaw, Sulphur Mines, West Hackberry (all in Louisiana), and Bryan Mound (Texas) domes will enable the national Strategic Petroleum Reserve to achieve its goal of storing some 750 million barrels of petroleum crude.

Since the time of the original site characterization, several new commercial exploratory wells have been completed, and DOE drilled 28 wells in 1983-85, preparatory to solution mining of the 14 caverns with an initial capacity of 11.5 MMBLS each. The new data do not preclude the possibility that space for five additional caverns may exist on the western and southern extensions of the 14 cavern locations. These extensions could be used for storage if additional exploratory drilling demonstrates suitable geometry and conditions within the salt mass. Additional storage space may also exist north of the 14 new caverns.

The new data presented in this report further substantiate the acceptability of this site and also refine the earlier geologic interpretation(SAND81-1045). Four earlier cross-sections through the cavern locations have been reinterpreted as a result of the geologic and geophysical data obtained from the cavern wells. Recommendations for exploratory drilling and logging are included for possible expansion caverns adjacent to the existing fourteen cavern locations.

2.0 GEOLOGY OF THE SALT DOME

2.1 Geological Interpretation

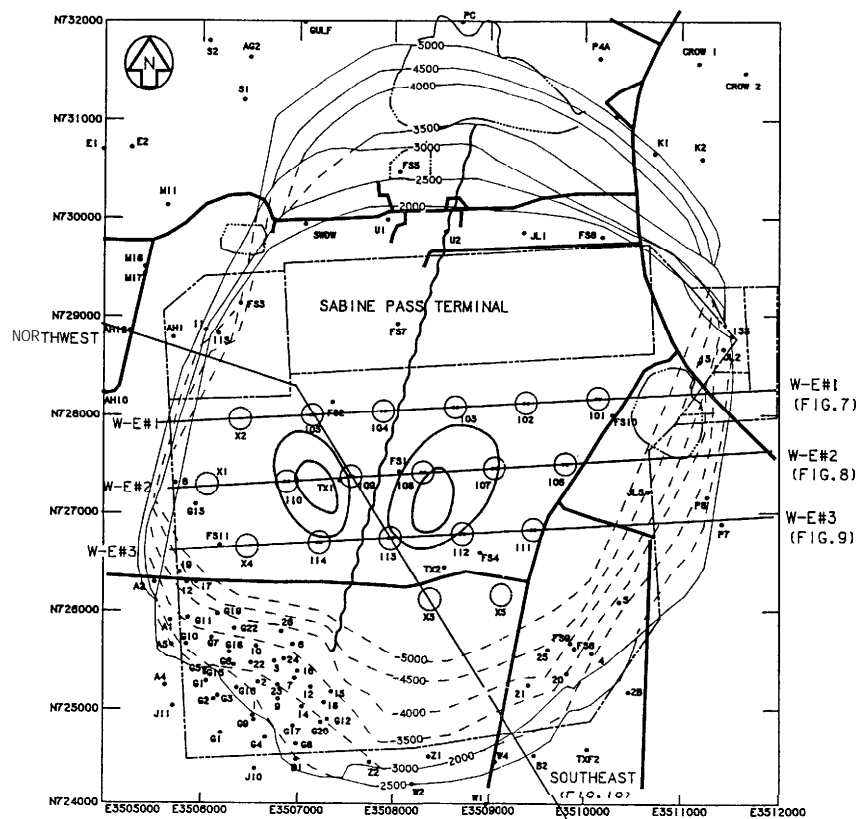
Revisions to the interpretation of the external geometry of the salt stock would not be useful, primarily because new drilling has been very limited around the dome in recent years and no other information exists that would change the interpretation presented in SAND81-1045 (1981). Amoco has drilled two additional wells downdip in the productive fault block at the southwest corner of the dome; they do not change the interpretation of the salt face, and the basic structure and stratigraphy have not been modified outside the salt. A summary geologic description of the Big Hill Salt Dome is included as Appendix A.

New information about the salt mass has come from the 14 double (28) wells that are being used for leaching the 14 new caverns (Figure 1). On-site geologic examination during drilling, geophysical logging, core examination and mineralogy, and quantitative geophysical log analysis provide the basis for interpreting the internal geologic structure of the dome in the report sections that follow.

2.2 Evaporite Mineralogy

2.2.1. Halite

The 4-inch diameter cores taken during the drilling of the cavern wells show that the halite at Big Hill is relatively pure and occurs in large, clear crystals, some over 5 ft on a side. The crystals are tightly interlocked, apparently as a result of the compaction due to the weight of the caprock, among the thickest in the Gulf Coast (Halbouty 1979). This coarse texture at Big Hill is shown in the core taken at -3507 ft in hole 106A (Figure 2). Halbouty (1979) described many examples of similar mineralogy; however, the exceptionally large and pure salt crystals seen in the Big Hill cores are virtually unique.



LEGEND

- U1, U2 UNION OIL LPG CAVERNS
- DRILL HOLE
- K2 LOCATION OF HOLE PENETRATING SALT
- SPR CAVERNS; X1-X5 CONNOTES PROPOSED EXPANSION CAVERNS
- 101
- DEPTH CONTOURS IN FEET, TO SALT
- PROPERTY LINE
- SECTION LINE
- ⊙ SPINE
- ~ SHEAR ZONE

500 0 500 1000
SCALE IN FEET

FIG. 1
BIG HILL SALT DOME
STRUCTURE MAP-SALT
SANDIA NATIONAL LABORATORIES
T.R. MAGORIAN
APRIL 1988



Figure 2 Core taken from 106A at -3507 ft showing single-crystal salt of exceptional purity.

2.2.2. Insolubles

The percentage of insolubles in the salt was calculated from the correlated anhydrite percentages, corrected for their composition, as shown by the density log. The amount of anhydrite increases as the edge of the salt is approached. Mapping in salt mines (Balk, 1949, 1953; Kupfer, 1962, 1974) has consistently shown an increase in anhydrite banding as the edge of a dome is approached. All accessible salt mines have been mapped and show this effect. In theory, also, the amount of insolubles should increase toward the edge of the intrusion. The calculated median of insolubles in all holes is 1.7%.

These percentages were calculated from the log density as a percentage of anhydrite assuming an apparent log density of 2.9, the rest being halite with an apparent log density of 2.0. The percent-feet of apparent anhydrite were then summed in a computer program; Appendix B shows the detailed data. The distribution of anhydrite is useful in defining internal dome structure, and in planning for disposal of insoluble materials during cavern leaching.

The largest percentage of anhydrite is found in wells 110A and B (Figure 1) which were drilled at the west edge of the dome between the dominant south overhang, and in a smaller overhang to the north of 110 in the middle of the west side of the dome, as shown only from one Amoco dry hole, Amoco 11.

Bands of insoluble anhydrite appear to parallel the edge of the salt. The usual form of these bands is shown in core from -5475 to -5480 ft from hole 106B (Figure 3). Broken chunks of anhydrite are also found as in core from 2527 ft in 106A (Figure 4). Massive anhydrite, larger than the core diameter, appears to be rare in this dome, but was found in core at -4510 ft in 110B (Figure 5).



Figure 3. Photo of core taken from 106B, -5475-80 ft, showing typical banded anhydrite.

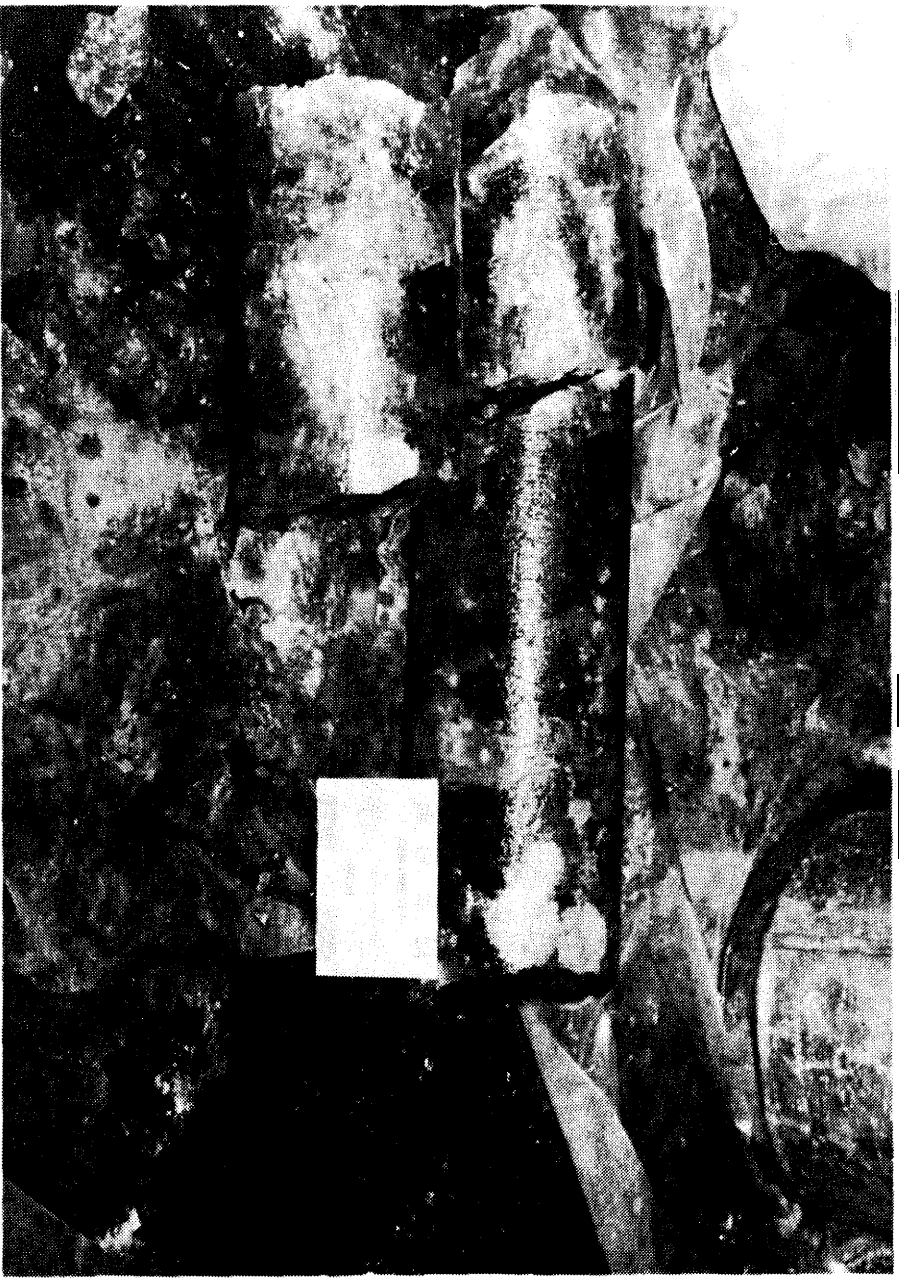


Figure 4. Photo of core taken from 106A at 2527 ft showing broken chunks of anhydrite.



Figure 5. Photo of core taken in 110B at -4510 ft showing massive halite (left) and crystalline anhydrite (scale in inches and tenths of feet).

2.2.3. Other Constituents

In addition to anhydrite, small quantities (5-20%) of sylvite (potassium chloride) were found in the southern tier of holes from 111 to 114 by x-ray diffraction of salt samples taken from the sidewall cores (University of Tulsa 1985). None of the cores showed any sylvite on visual inspection, but sylvite found by x-ray is finely disseminated. Widespread trace sylvite (<5%) was detected by x-ray diffraction in the southern tier of holes (111-114), but none was reported from the two other tiers.

Thus, sylvite, the second most commonly deposited evaporite constituent (after halite), appears to be confined to the edge of the dome out near the rim of the south overhang.

More than 5% sylvite was found only in:

- 111 at -1950 and -2252 ft depth;
- 112 at -2150, -3374, -3550, -3770, -3950, and -4309 ft;
- 113 at -4424 and -4462 ft;
- 113B at -1820 ft;
- 114A at -3902 ft;
- 114 at -2080 and -2700 ft.

2.3 Interior Structure from Well Logs/Core Validation

A unique opportunity to determine the interior structure of the intrusive salt was presented by the logs and cores available from the array of wells drilled to provide cavern storage at Big Hill. Current knowledge about the geometry of the interior of salt diapirs was previously obtained underground from salt mines, and from surface exposures in desert areas such as the Dasht-I-Kavir of Iran (Talbot and Jackson 1987) and the Paradox salt intrusives of Colorado and Utah.

The structure of salt flow in domes is visibly defined by the impurities. The principal impurity is anhydrite, found as thin bands folded and distorted by the intrusion. Thin bands of shale, sylvite and sand, and gravel are also found. This banded structure is the key to mapping salt mines in detail using the Cloos method for the study of intrusions, as applied to salt domes by Balk (1949, 1953) and Kupfer (1962, 1974).

In this report, we have extended the same type of structural analysis to well data obtained from the 28 holes drilled in the salt dome preparatory to leaching 14 caverns for the storage of crude oil. This is the first known example of the structural study of a dome from subsurface well data, as prior investigations were limited to mine observations.

2.3.1. Spines

The "spine theory" of salt intrusion holds that salt diapirs do not rise as a uniform mass, but move differentially as spines or tongues separated by shear zones (Talbot and Jackson 1987). These concepts have been applied to numerous Gulf Coast mines and are reviewed in the Weeks Island SPR Geological Site Characterization Report (SAND87-7111). The interpretation and correlation of the well log data suggest two spines separated by a shear zone occur in the south half of Big Hill dome, which is used by the SPR. The spines appear as anticlinal features or domes in the anhydrite correlation data (Figure 1; Appendix B). Alternative explanations of internal movement (Talbot and Jackson 1967) suggest flow of salt in continuous-flow bulbous shapes, whereby boundary shear zones are incorporated in the diapir. Our data are insufficient to favor either model.

2.3.2 Shear Zone

The shear zone, postulated to occur between the two spines, is evidenced as a sharp trough or low in the anhydrite correlation data. It exits in the dome overhang just east of 114, is found between 108 and 109, and between 103 and 104, as shown on the east-west cross-sections (Figures 6-9). The evidence for two separate spines is quite strong, since both

have a concentric pattern of mappable anhydrite bands, as shown by every usable log. Thus, the low between the spines is interpreted to be a shear zone, because of the basic geometry, and because shearing is evident in this structural position in all mapped salt mines that have spines.

The shear zone correlates very closely with the fault-bounding petroleum production zones under the southern overhang and with the edge of the Hackberry Embayment. As a result, we believe that this shear zone runs the length of the salt ridge and represents the master fault within the salt dome.

The smaller WNW-ESE cross fault (marked F7 on Figure 5-34 in SAND-81-1045) is apparently a secondary shear zone normal to the master fault that intersects it over the center of the dome, assuming Big Hill is similar to Weeks Island, for example. The subtle valley at Big Hill trending west-northwest may also reflect this underlying structure. However, the smaller diameter and greater overhang of Big Hill suggest that the secondary shear F7 may be hard to find within the dome. F7 apparently controls the small northwest, overhang which is so poorly defined. It should cross the salt just northeast of Cavern 101. Expansion into the Sabine Pass Terminal property (see Section 3.1) may be influenced by these possible shear effects along F7.

2.3.3. Salt Ridge

The shear zone parallels the alignment of domes from High Island through Big Hill to Spindletop. As discussed at various times by Hanna (1926), Levorsen (1954), and Halbouty (1979), this is an underlying salt ridge, which is parallel to the edge of the Hackberry Embayment and is the most prominent Frio feature of the Gulf Coast (see Appendix A).

The overhang, which underlies and limits the caverns on the south side of Big Hill, is 60" from the horizontal. It represents the equilibrium in the intrusive salt between the sands being deposited from the northwest and the Hackberry Embayment to the southeast.

2.3.4. Dome-Related Faulting

The shear zone postulated on the basis of information in the new wells continues outside the salt as the single petroleum-productive radial fault on the dome. This shear zone also represents the axis of the salt ridge on which Big Hill dome sits (see Appendix A). Virtually all domes studied reveal that shear zones are centered and parallel to the underlying salt ridges.

Although Big Hill lies at the south end of a large trend of Frio production, the oil accumulation against the salt adjacent to well 114 is primarily Lower Miocene, indicating vertical migration along active faults. It is bounded by this shear zone or fault and a tangential fault that parallels the overhang.

2.4 Caprock Geology and Hydrology

Only in the Cavern 106 wells at the east edge of the dome does the density log not support the caprock depth picked by the well-site geologist during drilling. Our analysis of the logs now available suggests that the top of the cap is between -250 and -300 ft MSL (Mean Sea Level) in 106 (Figure 8).

The caprock top was originally picked in 106 to be on the top of the massive carbonate, a correlative unit within the caprock that can be traced all the way across the dome at approximately -550 ft MSL. This unit is a dense but cavernous lime marker with a distinctive triple signature on electric logs. It appears at 584 ft depth on log 106B (-556 ft MSL).

The overlying unit, although softer interbedded lime and sand, apparently correlates with normal caprock in adjacent logs. Drill Hole 106 also shows the only temperature anomaly, indicating groundwater movement toward the edge of the dome. This indicates that the holes are located in the steep outer edge of the cap where more rapid gravity drainage is to be expected (Figure 6).

2.4.1. Caprock Faulting

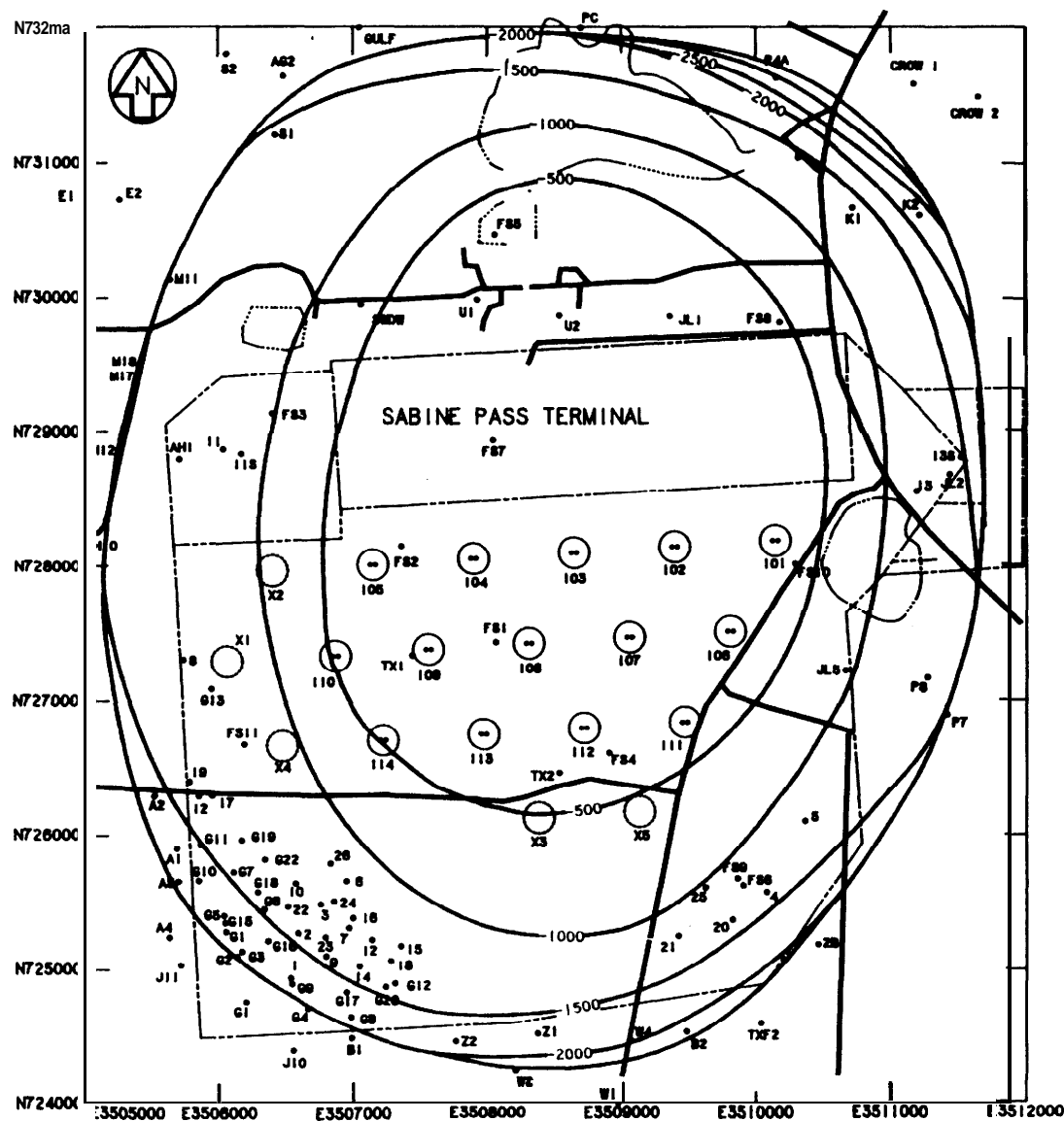
The shear zone found between the caverns (as seen in the pattern of banding in the insoluble components) is not only a fault on the southwest corner of the dome where it bounds oil production (Figure 1), but it also appears to have broken the caprock with a displacement of as much as 100 ft on the top of the cap and of the anhydrite.

The caprock is complexly faulted in virtually all the cores that have been recovered, so much so as to be a permeable jumble of broken blocks with secondary calcite cementation. This fault pattern is apparently manifested as the axial break along the crest of the underlying salt ridge bounding the Hackberry Embayment.

The displacement of the cap where the fault occurs appears to be down to the east (Figures 7-10), which is in accord with its origin along the basin rim. The top of the salt does not show this fault displacement because it is a solution interface controlled by groundwater salinity and influx of meteoric water.

2.5 Cross-Sections Through Caverns

Cross-sections (Figure 7-10; Table 1) have been revised from SAND81-1045 (1981) to show the new data and to transect the array of the new caverns. The three east-west cross-sections have been modified to include actual caprock and salt top depths encountered (very close to predicted) and internal salt data from the cores and density logs. The anhydrite correlations are drawn on these sections and on the salt map (Figure 1). The correlations are based on the values listed in Appendix B.



LEGEND

- U1, U2 UNION OIL LPG CAVERNS
- E3 DRILL HOLE
- K2 LOCATION OF HOLE PENETRATING SALT
- SPR CAVERNS: X1-X5 CONNOTES PROPOSED EXPANSION CAVERNS
- 101
- DEPTH CONTOURS IN FEET, TO CAPROCK
- - - PROPERTY LINE

500 0 500 1000
SCALE IN FEET

FIG. 6

BIG HILL CAPROCK DOME
STRUCTURE MAP-CAPROCK

SANDIA NATIONAL LABORATORIES

T.R. MAGORIAN

APRIL 1988

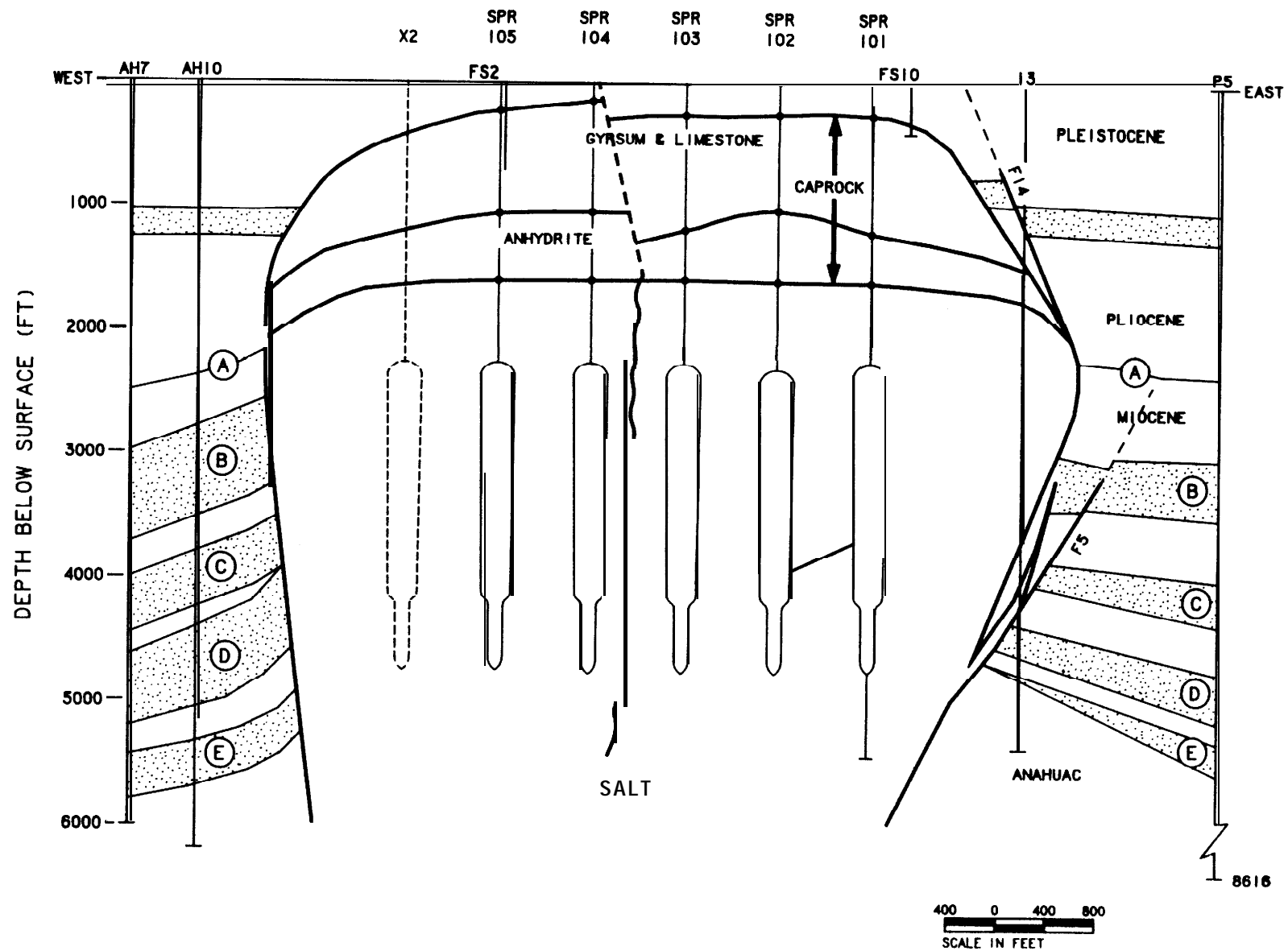


Figure 7. West-East cross-section No. 1, Big Hill Salt Dome; T. R. Magorian, April 1988. Stratigraphic units are explained in Table 1; anhydrite correlations between caverns are shown in Appendix B.

TABLE 1
Big Hill SPR Site Tertiary Geologic units

Age	Formation	Cross-Section Symbol	Stratigraphic Unit	Biostratigraphic zone	Sediment Type	Depositional Environment	Transprt Mode	Comment
Pliocene	Goliad	PL			Sand Over Clay	Alluvial Levee and Backswamp	River Channel	
				Buliminella	Sand Over Shale	Alluvial Levee	Silty Mud/Overbank	
Miocene	Fleming (Miocene)	A	Clovelly		Sand	Delta	Distributary Channel	
	Largarto	BF	Largarto	Bigenerina Florida	Shale	Backswamp		
	Oakville	B	Duck Lake	Bigenerina Humblei	Sand	Delta	Beach/Bar	Highly Mineralized Close to Salt
		AB		Amphistegina B	Shale	Marine Transgression	suspended Mud	Major Unconformity
	Catahoula	C	Duck Lake		Sand	Delta	Distributary Channel	
		RL		Robulus L	Shale	Marine Transgression	Suspended Mud	
	Main	D	Napoleonville	Discorbis Bolivarensis	Sand	Delta	Shoreline Beach/Bar	Main Producing Sand
		SD		Siphonina Davisi	Shale	Marine Transgression		
	Lower	E		Planulina Palmerae		Delta	Distributary Channel	
Oligocene	Anhuac	DR		Discorbis "restricted"	Shale	Deep Water	Pelagic and suspended Mud	Overpressured
		M		Marginulina	Thin Erratic Sand	Shelf Edge	Turbidity Current Proximal End	Slumps
	Frio	F	Upper		Sand	Deep Water	Turbidity Current	Slumps
	Frio		Lower	Hackberry Assemblage	Sand	Deep Water	Turbidity Current	Slumps Near Lithostatic Pressure

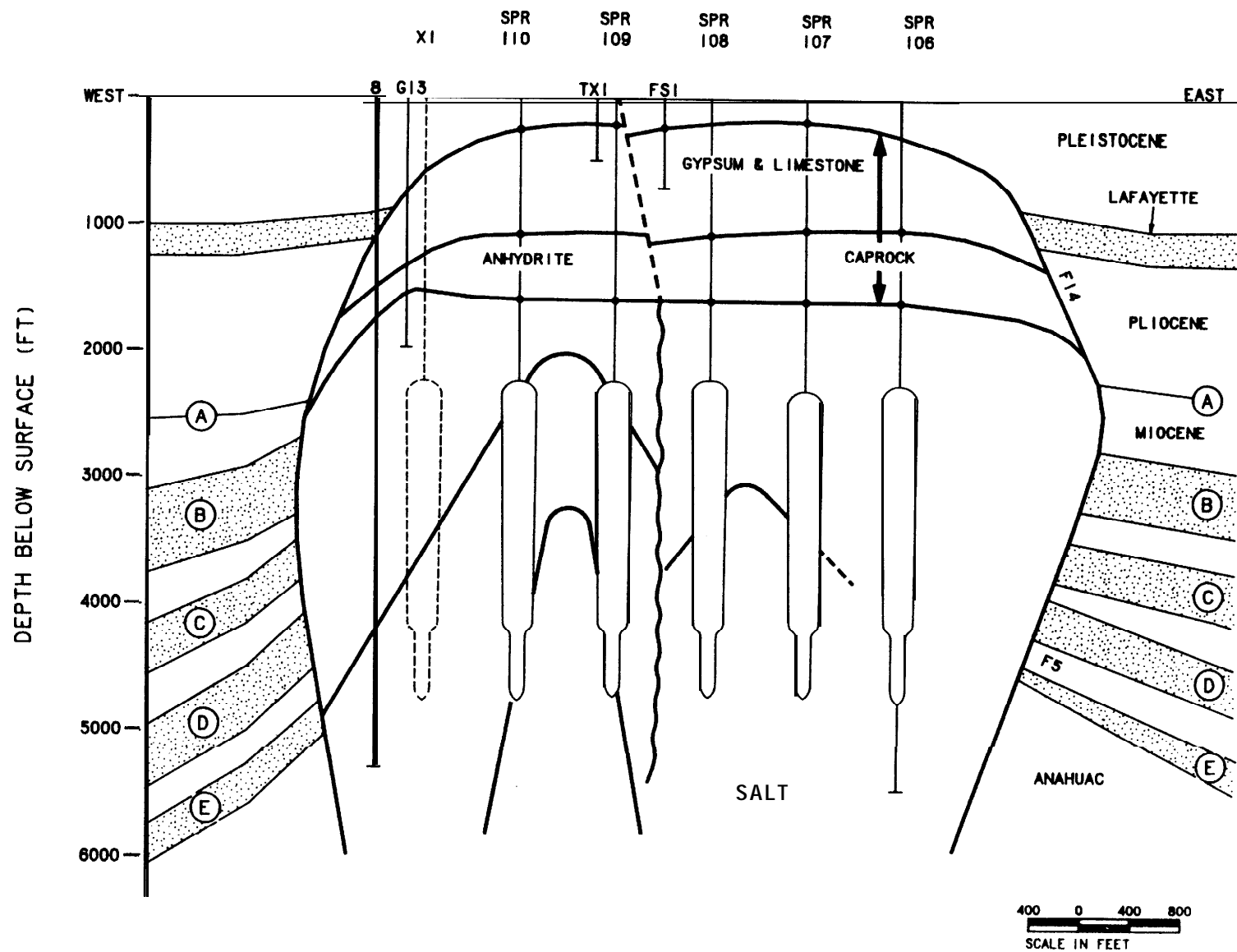


Figure 8. West-East cross section No. 2, Big Hill Salt Dome; T. R. Magorian, April 1986
 Stratigraphic units are listed in Table 1; anhydrite correlations between caverns are shown in Figure 9.

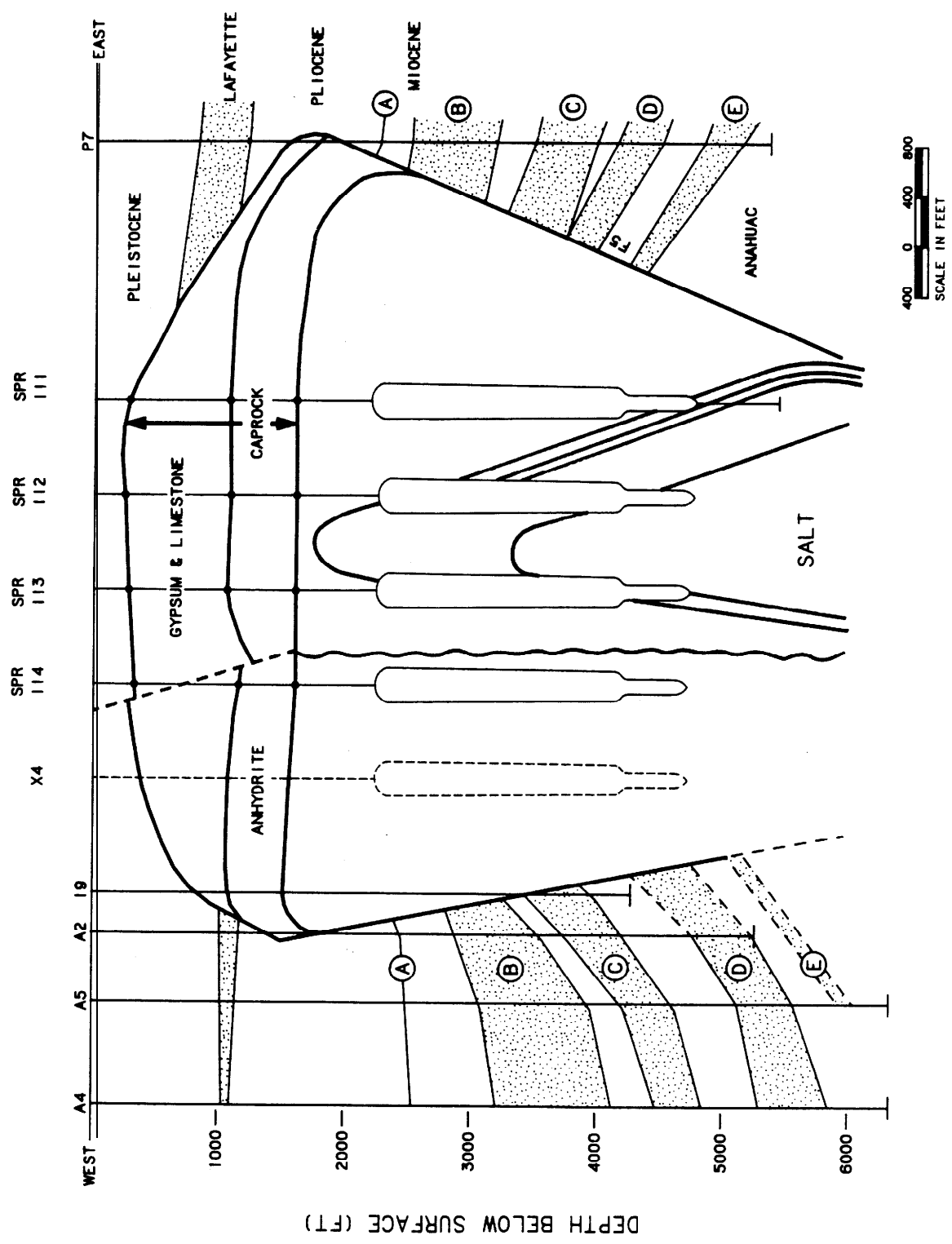


Figure 9. West-East cross section No. 3, Big Hill Salt Dome; T. R. Magorian, April 1988. Stratigraphic units are listed in Table 1; anhydrite correlations between caverns are shown in Appendix B.

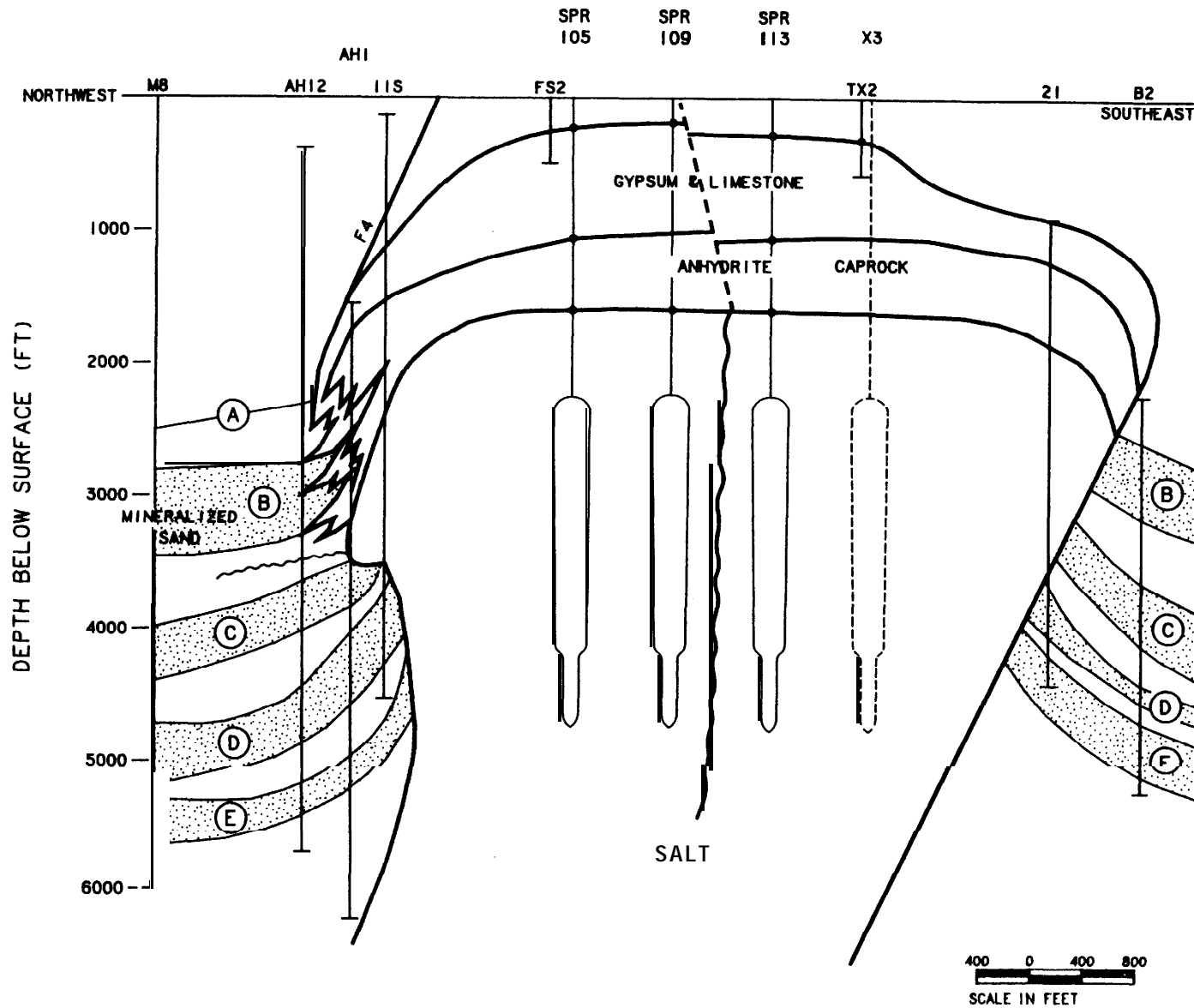


Figure 10. Northwest-Southeast cross section, Big Hill Salt Dome; T. R. Magorian, April 1988. Stratigraphic units are listed in Table 1; anhydrite correlations between caverns are

3.0 POTENTIAL EXPANSION AREAS FOR ADDITIONAL STORAGE

3.1 Cavern Layout

In SAND81-1045, it was reported that space for five caverns might exist adjacent to the 14 present locations along the western and southern periphery of the dome (locations x1-5, Figure 1). Lack of exploratory information in 1981 precluded confirming the suitability of this area. Because no significant new information has become available outside the dome since then, any additional caverns along the western or southern edges of the storage field will require exploratory drilling to establish their suitability.

Should requirements develop for considerable amounts of additional storage, serious consideration should be given to acquiring the Sabine Pass Terminal property north of the DOE property. The terminal project is now in abeyance and the site is available. This area is well within the -2000 ft salt contour and not overhung, as is the area south of the SPR site.

3.2 Exploratory Measures for Expansion of Caverns

In view of the previous success with and minimal expense of deepening wells for the corner caverns (101, 106, 111, 114) to prove sufficient salt exists along the overhang, this exploratory method should be used in the future for any caverns planned on the south side, such as X3 to X5 as shown on Figure 1. If the edge of the salt is encountered, the caverns will have to be shortened.

In an overhang, the -5000 ft salt contour can help define the 500 ft web thickness of salt surrounding the caverns to the dome edge, which is the recommended thickness needed to protect against leaching through the salt into the surrounding sediments. (The -3000 ft contour similarly would represent the shallowest depth that would be critical for even small leached caverns, e.g., one million barrels or less.

Proposed expansion cavern X1 is contained within the dome as shown by Amoco well 8, although the distance to the known salt edge is not the ideal spacing. That is, the full 500 ft of salt to the edge of the dome cannot be assured based on the available data from this single hole. A small-diameter exploratory hole some 200 ft west of X1 and angled toward the dome edge would help establish the containment geometry and salt properties.

Cavern X2 will probably require additional land and exploration of the northwest overhang, which is virtually unknown. As logged in the Adams and Haggerty well 1, the base of the salt is so similar in depth to that in the Amoco well 11 that a very sharp reentrant in the salt mass is suggested. However, the amount of salt penetrated in the Adams and Haggerty well is so small that it may be a purely local effect at the very edge of the overhang (Figure 9). The sidetracks in the Amoco well reveal almost-vertical beds that do not penetrate salt again. This usually indicates the presence of a shale sheath, which is to be expected below the mid-Miocene nonconformity. Thus, a large area without storable salt may extend under the DOE property.

Because the shape of the northwest overhang may vary south of Amoco well 11, a hole at the junction of the salt contours and the property line would provide a much higher degree of assurance for the presence of a lateral salt seal needed to store oil at X2 than would deepening of the sump. Two additional small-diameter exploratory holes west of X4 and south of X3/X5 would similarly establish the containment geometry. These holes could be drilled at relatively low cost and could include some geophysical logging. Further specification of an exploratory program has not been accomplished here because expansion has not been a priority.

4.0 GEOTECHNICAL CONSIDERATIONS

4.1 Cavern Leaching

The concentration of anhydrite in near-vertical bands parallel to and near the edge of the dome tends to enhance the safety of the leach operation, since caverns will leach preferentially away from the edge in the presence of insolubles. However, the presence of minor amounts of sylvite in the southern tier of holes near the overhang may be grounds for moderate concern, because sylvite is more soluble than halite. However, with the limited occurrence of more than a trace (defined as 5%, the level of resolution of the x-ray diffraction analyses) and the fine dissemination of the sylvite, careful sonar mapping of these caverns should provide sufficient understanding to prevent leaching through the overhang.

4.2 Natural Hazards: Subsidence Effects

Anticipated subsidence in the storage area, caused by salt creep closure following cavern formation, should not lower the surface enough to cause flooding during hurricanes because the exceptionally thick caprock will probably distribute the subsidence over a large area of the dome. Also, collateral subsidence resulting from sulphur extraction or widespread hydrocarbon removal is not present as at other sites (Goin and Neal 1988; Neal 1988). However, a subsidence monitoring plan is still recommended, as at all sites. The data will be particularly useful in understanding subsidence originating in cavern creep closure and will not be complicated by secondary sources.

4.3 Lessons Learned: Drilling and Logging

4.3.1. Lost Circulation

The most cost-effective method of penetrating the Big Hill carbonate caprock was demonstrated to be drilling without return circulation. By using expendable mud or water to cool the bit, a hole can be made in this cavernous, broken rock without having to emplace cement every few feet, once surface casing is set in the top of the hard carbonate caprock (upper caprock unit).

4.3.2. Hydrogen Sulfide (H₂S)

This toxic gas, commonly known in oilfield terminology as "sour gas," is formed in the reaction of hydrocarbons with anhydrite to form carbonate caprock and sulfur. Although sulfur exploration at Big Hill was not commercially successful, there are abundant shows of sulfur at the top of the anhydrite cap, particularly in the usual location near the rim of the dome. Big Hill is surrounded by domes that have produced commercial sulfur: High Island, Fannett and Spindletop (Myers 1968).

As a result, H₂S is detectable in most salt-dome caprocks (Dobbin 1935). SANDB1-1045 (1981) pointed out that H₂S can always be expected in salt dome drilling. H₂S was encountered in the aquifer above the caprock and reported to be present in the caprock fluids; however, no analyses were made by the drilling contractor to determine H₂S concentrations and locations. Atmospheric concentrations were detected around water tanks by safety personnel using "sniffers" and reported to be in the 20-30 ppm range. Drilling operations when H₂S is present require appropriate drill string, casing, drilling muds and safety precautions.

4.3.3. Well Logging and Coring

The coring program was satisfactory in determining the salt's character. On the other hand, the logging program was only partially satisfactory in the overburden and caprock; however, within the salt the gamma ray, sonic and neutron porosity (contact tools) did not perform as desired. Some logs above the salt were of poor quality and presumably had been affected by salinity. Poor contact with the formation walls is believed to be the reason for inferior log quality. Logging tools nominally designed for use in three inch holes, even when centered do not perform well in 13 5/8 inch and larger holes, even though marginally useful results are sometimes obtained.. Failure of the gamma ray logs may have resulted from improper gain settings.

The interpretation presented in this report is based on the density log alone, which prevents detailed separation of other insolubles from anhydrite. Fortunately, very little shale or sylvite was present in the core, based on visual observation. Only those logging tools that can directly contact the walls of these large diameter holes should be used in similar future operations.

5.0 SUMMARY AND CONCLUSIONS

The 28 wells drilled at Big Hill in 1983-85 preparatory to leaching the 14 new SPR caverns have provided new information to augment the 1981 geological site characterization report (SANDB1-1045). The following conclusions can be summarized:

- 0 The original structural interpretation is further validated, but the top of the salt is flatter than thought previously, deviating only slightly from -1600 ft MSL.
- 0 The percentage of anhydrite, as determined from density logs and core examination, averages about 1.7%. Minor amounts of more soluble sylvite occur in the southern tier of caverns and could affect cavern dimensions. Near-vertical anhydrite banding along the southern tier may provide an added solution deterrent between the dome edge and caverns.
- 0 Anhydrite bands are correlative between drill holes, showing that at least two spines, separated by a southwest-northeast shear zone, exist within the salt mass.
- 0 The shear zone displaces the caprock down to the east by as much as 100 ft.
- 0 The shear zone is aligned with the High Island-Spindletop salt ridge and is parallel to the Hackberry Embayment, a major structural/-depositional feature.

- Space for additional caverns west or south of the 14 new caverns is not confirmed, and exploratory drilling is needed to establish the suitability of this location. The Sabine Pass Terminal Property immediately north of the DOE property should be considered if exploration alternatives are desired.
- Because of the deep and exceptionally thick caprock, subsidence should not be a serious future concern, but monitoring should be performed nevertheless. Verification of creep models can be advanced with these data.
- Lessons learned during drilling include:
 - penetration of carbonate caprock was effective with water or mud and using no return circulation;
 - H₂S was reported in caprock and groundwater above caprock;
 - Logging tools require direct contact with sidewalls to perform satisfactorily. Saline water may have affected measurements above the caprock.

APPENDIX A.
SUMMARY OF BACKGROUND GEOLOGIC INFORMATION
(FROM SANDU-1045)

A.1. General Aspects

Big Hill salt dome is located some 20 miles southwest of Port Arthur, Texas, and five miles north of the intracoastal waterway. The dome rises to 37 ft MSL, some 27 ft above the surrounding grass-covered and scattered forest land. The dome originated from the buoyant rise of the deeply buried Jurassic Louann salt, like other Gulf Coast salt domes. The dome is within the Gulf Coast Geosyncline, a depositional basin characterized by thousands of feet of sands and shales of Pliocene, Miocene, and Oligocene age that overlay the mother salt, occurring some 30,000 ft below sea level.

The dome is generally cylindrical, rising to about 1600 ft below MSL in the vicinity of the SPR caverns. The east and west sides of the dome are nearly vertical, but the south side is overhung below 2000 ft at a dip of about 60 degrees. The north side dips gently downward to about 2000 ft and then increases to 60 degrees between 2000 and 10,000 ft.

A.2. Geologic History

The Gulf Coast geosyncline was one of a string of rift basins created by the opening of the Atlantic about 200 million years ago (mya) in the breakup of Pangaea, the single massive continent that had drifted together at the end of the Paleozoic (-240 mya).

The initial deposits underlying the salt are oceanic basalts and red beds of Triassic (-215 mya) age, called Eagle Mills in the Gulf Coast and Newark Series in New Jersey where they are best exposed. These beds are deposited, where known, on metamorphosed Paleozoic rocks like those found in the core of the Appalachian Mountains.

The more extensive overlying redbeds of early Jurassic (-180 mya) age are called the Norphlet Formation on the Gulf Coast. The original depositional basin of the Jurassic salt and evaporites was one of this string of rift-valley dry lakes, like Death Valley today, which is on the extension of the East Pacific rise into California and Nevada.

The anhydrite on top of the Louann Salt is called the Buckner Formation, and the overlying dolomite is known as the Smackover Formation, the Gulf Coast correlative of the Arab Limestone pay of the Persian Gulf, the most productive single petroleum horizon in the world. The remainder of the overlying Jurassic consists of a thick sequence of Cotton Valley limestone and bituminous shale.

The lower Cretaceous (-125 mya) sequence of Hosston elastic and limes, Sligo oolites, Pine Island Shale, James lime reef, Ferry Lake Anhydrite, and Glen Rose limes are overlain unconformably by the upper chalk section: Austin, Ozan or Annona, and Nacatoch or Arkadelphia with intervening Blossom or Tokio sands and thick shales. The shallow-water reef carbonates are equivalent to basinal shales to the south which probably underlie Big Hill.

The Tertiary (65-3 mya) sequence consists of Midway shale, Wilcox deltaic deposits (including coals that have been penetrated near Big Hill in Jefferson County, Texas) and Yegua shales and sands, all overlain by Vicksburg-Jackson shale and Frio sands, the deepest penetrated near the dome.

:

The salt from which the High Island - Spindletop Ridge has formed is probably not in its original depositional position. It appears to have migrated southward and upward as a sill through the sediments described above, or outside to the seaward of the thick sediment wedge at a depth of two or three to six or seven miles. This sill is believed to be exposed at

the toe of the sediment pile on the floor of the Sigsbee Deep today (Humphris 1978). Because seafloor-spreading has revolutionized our concept of the origin of basins like the Gulf Coast, this concept of deep horizontal salt intrusion is most innovative and important.

Hackberry Embayment

Three of the domes chosen for the Strategic Petroleum Reserve are in and around the Hackberry Embayment: Big Hill on the salt ridge forming the west edge; Sulfur Mines on an east-west ridge with Edgerly Dome near the north edge; and West Hackberry, which is the type section of the Hackberry shale and lies in the middle of the embayment. The Hackberry is an over-pressured organic-rich shale in the Middle Frio (upper Oligocene -30 mya) equivalent in age to Marzinulina texana sands found outside the embayment. Turbidite sands near the mouth of channels along the edge form isolated stratigraphic traps, some of the few in the Gulf Coast. Unlike the Houma embayment of middle Miocene (-15 mya) age (but like the Nodosaria embayment, which includes Bayou Choctaw dome), the Hackberry embayment is rich in salt domes.

The overall result is that the Gulf Coast is one of the largest sedimentary basins in the world, extending from Mexico to the Appalachians, and being thickest at the mouth of the Mississippi, the world's second largest river system. The largest is the Amazon, which is related to two oil-productive sedimentary basins: the elastics, which have accumulated at the foot of the Andes in Ecuador and Peru, and the rifted Atlantic basin, once fed by the Amazon and now the delta of the Niger.

Large oil accumulations have been found associated with smaller river systems where salt and anhydrite overlie the oil source rocks, such as reservoirs in Saudi Arabia and West Texas, for example. This favorable geometry is found in the Cretaceous sediments of the inner Gulf Coast in East Texas and North Louisiana under the Ferry Lake anhydrite, although salt is a much better seal.

The asymmetric overhang at Big Hill dome is a much less complete seal, requiring lateral sealing along the shear zone, which has acted as a fault beyond the edge of the salt stock. It is not certain, however, that all the oil and gas trapped against this salt dome have been found. As seen in the wellfield distribution on Figure 1, the oil occurs mainly along the southwestern edge of the overhang, but considerable amounts are also found off the dome to the northwest. Cumulative production through 1979 was some 15 million barrels.

The asymmetry of the southern overhang is also a factor in emplacing the SPR caverns. At depth, the dome may contain impurities or structural discontinuities that could affect cavern leaching and integrity.

Major regional (growth) faults occur north of the site, and the domal uplift has created tangential and radial piercement faults. A shear zone through the dome is aligned with the underlying salt ridge and with domes from High Island through Spindletop. This ridge parallels the edge of the Hackberry embayment, the most prominent Frio feature of the Gulf Coast.

APPENDIX B,
ANHYDRITE CORRELATIONS

This is apparently the first time that the structure of a salt dome has been mapped from well control, using the model found in mines by Balk and Kupfer. Because the intrusive structure of the salt is near vertical, only closely-spaced wells can be used.

The neutron density device was the only logging tool working in these large holes, since no wall contact was achieved. In a few badly washed out areas, no data were recorded. These correspond with some of the twistoffs of the drill string which on fishing found the hole to be over four feet across. The neutron density logs were correlated inside the salt showing each anhydrite bed.

Thicknesses of anhydrite layers are shown in Table B-1. Only those indicated are used for correlation, numbered within and lettered between, caverns. These thicknesses arbitrarily represent a mean of 9% anhydrite as measured on the density log over the footage shown in the table.

The method used and characteristic layer log-response are shown in Figure B-1. Each group of approximately a dozen distinctive anhydrite bands could be correlated between the A and B well of each cavern only 40 feet apart. Each correlative group is numbered sequentially down from the casing seat to total depth of the shallower hole.

The correlations are surprisingly good, in fact, complete except where sharp bends, knees or kinks obviously occur, as shown by the distortion of the log peaks. Those particularly-distinctive bands that could be correlated with the next cavern 750 feet away are shown with a correlation letter in sequence for the entire site. The positions of these marker beds are shown in each cavern in Figure B-2.

The average percentage over the entire depth logged in salt of each hole is shown in Table B-2. These were averaged to calculate the total percentage of anhydrite to be leached. This represents most of the insolubles which can accumulate in the brine pond and line to the Gulf.

HOLE A				HOLE B			
DEPTH TO TOP OF ANHYDRITE	THICKNESS FT.	CORRELATION		DEPTH TO TOP OF ANHYDRITE	THICKNESS FT.	CORRELATION	
		CAVERN	SITE			CAVERN	SITE
2233.5	4.1			2164.1	11.4		
2467.8	4.0			2234.3	15.5		
2516.8	5.6			2504.0	9.3		
2577.6	3.8			2735.1	11.6		
2743.4	8.0			3025.4	8.6		
2774.7	12.3			3099.7	24.3	3	
3187.8	15.3			3125.9	11.5		
3245.5	6.7			3139.0	19.2		
3321.8	6.7			3210.4	12.1	4	
3329.8	10.2	1		3240.9	12.2		
3385.7	6.4			3261.0	10.8	5	
3396.2	12.5	2		3273.1	8.3		
3447.7	14.8			3364.4	10.9		
3485.9	21.9	3		3430.8	10.5		
3545.4	8.7			3480.9	5.2		
3562.0	12.3	4		3563.3	8.4		
3579.9	14.8			3752.7	22.3		
3660.3	12.1	5	E	3818.4	5.5		
3796.8	9.2			3828.6	9.6		
3926.8	13.5			3847.2	14.8		
4282.0	15.8			4018.5	13.4		
4365.0	6.5	6		4082.3	9.4		
4437.1	10.5	7		4114.8	16.3		
4497.1	26.9	8	B	4145.9	23.9		
4575.6	17.2	9		4257.4	27.6	6	
4670.4	14.8	10		4286.4	15.1		
4686.1				4338.6	21.4		
				4400.8	21.2	8	
				4436.1	11.5		
				4475.5	12.3	9	
				4543.6	10.9		
				4563.6	17.2	10	
				4615.4	8.4		
				4652.7	11.8		
				4752.0	8.6		
				4874.9	22.3		
				4940.4	12.5		
				5004.4	8.1		
				5081.8	12.7		
				5447.1			

TABLE B-1

CAVERN 102					
HOLE A			HOLE B		
DEPTH TO TOP OF ANHYDRITE	THICKNESS FT.	CORRELATION CAVERN SITE	DEPTH TO TOP OF ANHYDRITE	THICKNESS FT.	CORRELATION CAVERN SITE
2299.1	23.5		2310.5	16.5	
2405.5	22.4		2344.7	6.7	
2554.9	15.1	1	2416.9	7.7	
2571.2	5.4		2431.3	14.9	
2631.1	10.6		2478.4	14.4	1
2643.8	11.6		2494.3	8.5	
2665.3	13.4	2	2538.4	2 \geq \geq	
2735.9	11.3		2576.2	\geq 6	
2763.3	10.4		2586.4	11.5	
278 \geq 1.7	16.7	3	2603.5	12.2	2
2858.7	20.1		2641.6	\geq 2	
2930.3	12.8	4	2666.5	7.2	
3002.4	16.1		2737.7	13.8	3
3028.4	6 \geq		2855.8	26.5	4
3167.9	10.6		2886 \geq	17.8	
3266.5	38.2		2969.5	15.8	
\geq 412.3	15.7		3513.6	28.1	
3621 \geq	20.3		3580.4	16.6	
3667.8	18.1	5	3618.0	12.4	5
\geq 701.7	12.6		3693.5	16.4	
3770.3	9.1		3799.4	23.7	
3794.1	8.1		3861.2	8.6	6
3830.9	16.8		3871.7	16.5	7
3906.6	6.8	6	3908.7	20.9	
3918.2	6.0	7	3983.2	21 \geq	8
4013.1	9.9	8	4015.4	25 \geq	
4049.2	12.0		4259.2	16.5	
4096.5	16.1		4429.0	10.7	
4136.2	24.7		4700.3	17.3	
4170.9	8 \geq		4768.5		
4259.1	9.1				
4321.2	12.0				
4351.3	17.0	9			
4379.2	16.0	C			
4739.7					

TABLE B-1

CAVERN 103

HOLE A				HOLE B			
DEPTH TO TOP OF ANHYDRITE	THICKNESS FT.	CORRELATION		DEPTH TO TOP OF ANHYDRITE	THICKNESS FT.	CORRELATION	
		CAVERN	SITE			CAVERN	SITE
2525.3	30.1			2972.4	22.3		
2627.6	28.0			3025.6	21.5		
2767.5	9.5			3048.7	17.8	1	
2936.6	7.9			3084.0	20.1		
2948.3	11.8			3160.0	16.2		
3017.8	12.2			3250.1	20.5		
3226.5	18.0	1		3440.7	10.3	2	D
3370.7	14.9			3570.0	23.4		
3440.2	7.0			3734.8	29.5		
3562.2	12.7	3	E	3838.6	19.4	5	
3617.6	17.3			3935.5	7.7	6	
3647.9	14.7	4	F	3955.7	12.8		
3930.4	24.1	5		3970.0	14.3	7	
4001.4	7.6	6		4310.8	18.5		
4057.2	16.3	7		4605.7	15.5		
4096.3	16.7			4629.9	14.5		
4196.1	20.3	8		4706.6	14.4		
4268.5	11.0			4766.6			
4646.2	14.6						
4750.8							

TABLE B-1

CAVERN 104							
HOLE A				HOLE B			
DEPTH TO TOP OF ANHYDRITE	THICKNESS FT.	CORRELATION		DEPTH TO TOP OF ANHYDRITE	THICKNESS FT.	CORRELATION	
		CAVERN	SITE			CAVERN	SITE
2381.3	14.6			2743.1	23.2		
2397.1	6.2			2884.3	33.4		
2450.7	65.4			3028.9	13.3		
2586.3	20.7			3069.7	26.5	1	
2627.4	12.6	1		3097.3	22.1		
2711.0	15.6	2		3123.3	25.3		
2761.3	23.9	3		3162.6	21.4	2	
2814.5	18.2			3198.0	28.5	3	G
2924.4	17.1			3228.3	19.5		
2981.5	40.2			3261.7	18.6		
3102.7	22.1			3320.0	20.3		
3206.2	28.5			3430.1	24.9		
3313.1	21.3			3556.1	20.9		
3619.9	5.0			3603.7	8.9		
3688.3	11.4			3636.9	16.7		
3837.4	11.8			3678.3	11.9		
3916.5	23.5			3733.7	20.4		
4144.3	29.7			3828.7	22.3		
4270.6	13.1			3905.3	14.5		
4322.8	13.2			4004.2	7.9		
4375.7	9.8			4030.6	28.5		
4462.6	26.9			4137.4	20.1		
4757.4				4159.6	21.9		
				4240.7	23.4		
				4670.0	11.8		
				4776.0			

TABLE B-1

-----CAVERN 105-----						
HOLE A				HOLE B		
DEPTH TO TOP OF ANHYDRITE	THICKNESS FT.	CORRELATION		DEPTH TO TOP OF ANHYDRITE	THICKNESS FT.	CORRELATION
		CAVERN	SITE			CAVERN SITE
2297.6	15.3			2461.3	8.6	
2340.6	11.3			2500.7	12.4	
2354.9	8.6			2516.4	10.8	
2406.1	29.2			2589.8	14.1	
2506.3	8.6			2673.4	21.3	
2540.3	8.5			2740.8	22.7	
2578.6	9.2			2815.3	11.5	1
2595.3	14.7			2871.3	11.8	2
2622.5	19.4			3010.3	25.5	
2656.0	9.6			3059.7	14.3	
2668.8	4.7			3107.1	11.4	3
2699.1	14.0			3172.8	14.7	
2726.5	9.6			3189.0	16.4	4
2740.3	19.4	1		3477.6	22.3	
2772.9	15.3	2		3502.1	8.3	
2807.2	10.5			3772.7	28.4	
2819.0	8.1			3937.5	6.4	
2840.9	10.3			4126.9	15.4	
2867.8	15.2			4716.3		
2945.2	12.8					
3001.6	20.1	3				
3036.9	16.3					
3068.4	8.2					
3113.0	18.6	4				
3138.3	14.0					
3165.4	22.5					
3204.1	9.5					
3253.2	10.5					
3287.3	12.1					
3301.7	26.5					
3529.6	16.8					
3626.9	42.8					
3791.0	20.3					
3818.6	13.0					
3917.1	14.0					
3942.5	18.5					
4111.8	15.6					
4144.3	21.3					
4416.5	60.0					
4611.5	15.0					
4651.3	25.8					
4742.7						

TABLE B-1

CAVERN 106

SHEET 1 OF 2

HOLE A				HOLE B			
DEPTH TO TOP OF ANHYDRITE	THICKNESS FT.	CORRELATION		DEPTH TO TOP OF ANHYDRITE	THICKNESS FT.	CORRELATION	
		CAVERN	SITE			CAVERN	SITE
2230.8	10.9			2182.1	6.3		
2243.4	8.4			2224.4	12.1		
2253.3	10.5	1		2247.1	18.7		
2295.6	6.8	2		2306.9	13.7	1	
2467.3	8.6			2349.5	15.7	2	A
2510.5	11.1	3		2389.2	14.1		
2523.5	7.9	4		2447.7	7.4		
2553.1	6.4			2459.0	8.9		
2595.9	15.3	5		2504.7	13.8		
2627.6	10.4			2559.9	10.0	3	"O"
2658.2	10.9			2570.8	5.8	4	
2678.1	17.4			2583.0	13.8		
2706.3	9.0			2637.8	23.1	5	
2741.4	10.1	6		2706.8	5.1		
2757.1	9.3	7		2815.3	25.0	6	C
2776.6	8.2			2849.9	15.3		
2786.2	11.7			2949.5	6.3		
2831.7	13.4			2961.2	5.9		
2868.9	15.8			2968.7	11.0		
2892.4	24.7			2986.1	7.8		
2983.1	11.2			3006.2	7.6		
3185.2	9.2	8		3094.0	8.9		
3233.3	7.8	9		3117.9	12.3		
3287.5	15.9	10		3136.5	16.9		
3329.2	14.3	11	H	3210.5	5.8	8	
3347.5	9.5			3254.4	9.6		
3378.6	6.8	12		3265.4	5.7		
3411.1	16.2			3275.8	8.8	9	
3444.0	9.8			3288.9	15.5		
3471.9	9.0			3330.4	8.6	10	B
3503.6	12.4			3343.3	4.2		
3533.8	5.1			3366.6	12.0	11	
3558.7	13.5			3423.0	13.3	12	
3592.0	10.5			3452.9	10.2		
3615.7	5.7			3585.1	15.3		
3623.7	6.9			3673.2	5.8		

TABLE B-1

CAVERN 106

SHEET 2 OF 2

HOLE A				HOLE B			
DEPTH TO TOP OF ANHYDRITE	THICKNESS FT.	CORRELATION		DEPTH TO TOP OF ANHYDRITE	THICKNESS FT.	CORRELATION	
		CAVERN	SITE			CAVERN	SITE
3636.0	17.6	13		3686.8	12.9	13	
3702.1	13.8			3742.1	9.0		
3734.4	16.2			3767.6	15.5		
3754.6	7.4			3795.4	16.6		
3771.8	9.0			3891.6	12.0		
3808.0	14.7	14		3906.7	5.7		
3828.2	11.5	15		3969.2	14.9		
3849.5	12.0	16		3986.2	14.7		
4101.3	7.5			4018.6	18.6		
4246.0	6.9	17		4109.8	30.9		
4294.2	7.4	18		4151.4	12.6		
4323.1	8.3	19		4234.9	8.0		
4335.8	20.6	20		4251.8	18.9		
4360.9	9.9			4291.1	8.5		
4398.4	12.9			4304.5	8.2		
4460.3	10.0			4391.0	12.0		
4472.4	6.3	21		4407.5	9.3		
4480.1	7.3	22		4428.7	6.0		
4494.5	5.8			4517.1	11.6	21	
4508.6	7.6			4532.4	9.7	22	
4539.4	12.3	23		4565.2	13.5		
4568.8	18.4			4593.3	9.5		
4590.1	6.3			4605.2	6.9	23	
4607.2	7.4	24		4649.2	6.0	24	
4617.1	7.1	25		4656.5	5.0	25	
4641.3	14.2			4693.2	8.4		
4661.8	6.9			4708.4	5.7		
4680.5	6.6	26		4733.2	6.7		
4692.3	5.9	27		4759.1	8.3		
4699.6	8.0	28		4893.6	8.3		
4742.8				4915.7	8.6		
				5007.1	8.8		
				5026.2	13.6		
				5124.6	11.4		
				5163.3	17.2		
				5203.8	16.8		
				5264.0	8.3		
				5352.3	11.8		
				5473.8			

TABLE B-1

CAVERN 107							
HOLE A				HOLE B			
DEPTH TO TOP OF ANHYDRITE	THICKNESS FT.	CORRELATION		DEPTH TO TOP OF ANHYDRITE	THICKNESS FT.	CORRELATION	
		CAVERN	SITE			CAVERN	SITE
2297.7	12.6			2534.3	9.5		
2372.0	10.0			2585.2	14.2		
2853.8	10.9			2620.0	9.5		
2981.6	22.2			3141.1	5.6		
3144.0	15.9			3287.1	8.8	1	
3186.4	9.5	1		3428.4	8.5	2	
3232.0	21.2			3439.4	6.5	3	
3310.4	6.1	2		4001.0	8.0		
3318.7	7.7	3		4104.1	12.3		
3492.1	10.4			4142.2	20.9		
3546.9	23.1			4208.4	17.9		
4270.7	11.4			4338.3	7.1		
4295.1	13.3			4420.3	6.5		
4310.5	3.7			4644.1	8.0		
4384.3	18.3			4730.4			
4715.4							

TABLE B-1

CAVERN 108

HOLE A				HOLE B			
DEPTH TO TOP OF ANHYDRITE	THICKNESS FT.	CORRELATION		DEPTH TO TOP OF ANHYDRITE	THICKNESS FT.	CORRELATION	
		CAVERN	SITE			CAVERN	SITE
2187.4	10.9			2349.2	12.3		
2295.9	3.0			2415.5	14.6		
2345.9	4.8			2479.1	12.7		
2484.8	13.9			2498.8	12.3		
2500.6	14.2			2516.5	19.8		
2978.4	15.1	1		2626.3	9.4		
2995.1	16.7			2732.6	14.3		
3036.5	10.7			2802.6	12.6		
3048.3	10.4	2		2849.3	9.9		
3158.8	10.8			2887.2	8.5		
3181.3	9.3			3021.9	13.3		
3325.1	8.3	3	D	3048.3	9.3		
3336.7	7.9			3072.5	13.3		
3354.2	11.3			3114.5	15.4		
3492.3	13.4	4		3225.1	12.3	1	
3528.5	6.6	5		3239.2	21.8		
3564.7	6.1	6		3262.6	11.7		
3599.4	5.0			3285.6	11.9	2	
3696.1	40.2			3391.9	9.2		
3850.9	18.9			3537.7	11.3		
3888.8	10.2			3553.6	8.4		
3932.4	9.5			3565.3	14.3		
4003.8	20.2	7		3594.0	9.3		
4045.3	8.2	8		3646.9	5.9		
4056.8	6.0	9		3876.3	12.0		
4094.6	26.7	10		3948.1	16.3		
4283.8	9.0	11		3966.4	7.8		
4313.2	20.3	12		4179.4	13.6		
4381.6	35.9			4231.2	7.9		
4575.5	6.6			4246.2	11.1		
4713.3				4272.2	16.4	7	
				4290.8	11.5		
				4315.3	17.5	8	
				4334.0	16.9	9	
				4364.2	34.5	10	
				4617.6	11.3	11	
				4642.8	17.7	12	
				4727.3			

TABLE B-1

CAVERN 109

HOLE A				HOLE B			
DEPTH TO TOP OF ANHYDRITE	THICKNESS FT.	CORRELATION		DEPTH TO TOP OF ANHYDRITE	THICKNESS FT.	CORRELATION	
		CAVERN	SITE			CAVERN	SITE
2166.2	20.2			2266.3	13.7		
2204.2	10.2			2364.5	21.5	1	
2280.4	26.5	1	G	2638.3	14.9		
2323.0	16.2			2689.5	18.5	2	E
2577.3	22.7	2		2730.6	10.2		
2661.6	12.1			2773.0	26.6	3	F
2701.7	14.4			2847.5	20.1		
2793.0	8.5			2897.7	16.8		
2802.9	10.1			2963.7	20.5		
2818.2	23.8			2986.6	15.6		
2853.4	9.9			3004.6	14.5		
2865.4	10.7			3070.3	32.0	4	
2915.2	18.9			3155.4	27.1		
2935.8	12.8			3215.3	14.1		
3021.0	18.4			3255.4	16.7		
3046.6	12.9			3324.8	30.0	5	
3061.7	29.4			3392.9	14.4		
3096.4	8.1			3470.5	12.0		
3140.2	6.4			3510.3	9.7		
3218.6	16.0			3577.5	23.5		
3508.4	19.4			3650.6	17.9		
3538.4	15.5			3943.8	18.7		
3556.4	19.7			4169.0	17.3		
3777.4	12.8			4197.8	28.3	6	
3811.3	19.7			4340.1	13.0		
3882.3	22.1			4389.8	23.0		
3907.0	25.1	6		4551.6	31.1	7	
3934.7	9.9			4719.3			
4009.7	42.2						
4140.1	9.9						
4152.1	11.4						
4202.2	9.1						
4287.0	24.4	7					
4322.7	21.9						
4433.4	36.8						
4722.2							

TABLE B-1

CAVERN 110

SHEET 1 OF 2

HOLE A				HOLE B			
DEPTH TO TOP OF ANHYDRITE	THICKNESS FT.	CORRELATION		DEPTH TO TOP OF ANHYDRITE	THICKNESS FT.	CORRELATION	
		CAVERN	SITE			CAVERN	SITE
2147.1	20.6			2139.2	14.9		
2207.3	8.9			2178.0	19.5		
2218.1	21.0			2287.0	16.4		
2247.2	14.7			2311.7	12.4		
2350.2	11.0			2417.9	17.2	1	
2366.3	14.2			2472.7	7.2	2	
2406.4	19.4			2482.9	8.6	3	
2476.0	7.4			2497.3	12.4	4	
2503.1	31.2	1		2531.4	12.6		
2535.7	18.7			2553.4	19.7		
2585.8	9.0	2		2628.1	8.9		
2595.7	7.8	3		2642.5	5.7	5	
2606.3	6.7	4		2716.8	12.3	6	
2743.6	13.0			2761.2	16.1	7	
2770.6	14.3			2867.8	13.5		
2825.6	10.3			2908.5	18.7		
2838.2	10.1			2931.8	9.5		
2855.3	8.9			3162.4	7.9		
2868.3	10.2			3276.2	12.7		
2909.7	12.6			3477.2	15.1		
2945.0	15.0			3511.4	14.2		
2989.9	25.0			3564.5	17.7		
3072.2	17.5			3679.7	24.0	8	
3100.9	10.4			3705.9	16.7		
3126.5	10.3			3735.0	13.5		
3141.7	18.5			3790.0	10.1	9	
3234.3	15.0			3805.9	13.0	10	
3252.8	9.8			3821.4	10.0		
3265.1	11.0			3845.3	10.5		
3278.7	6.2			3941.9	14.3		
3300.1	7.7			4045.4	13.5		
3310.5	11.8			4061.3	13.8		
3361.0	38.3			4116.4	24.2	11	N
3462.2	17.2			4210.0	9.1	12	
3484.0	12.7			4230.7	11.0		
3513.4	8.8			4253.5	6.1		

TABLE B-1

CAVERN 110

SHEET 2 OF 2

HOLE A				HOLE B			
DEPTH TO TOP OF ANHYDRITE	THICKNESS FT.	CORRELATION		DEPTH TO TOP OF ANHYDRITE	THICKNESS FT.	CORRELATION	
		CAVERN	SITE			CAVERN	SITE
3560.5	14.2			4343.9	27.3	13	
3593.6	9.4			4395.4	18.3		
3615.5	17.0			4466.9	21.0	14	
3720.5	15.7			4507.6	14.1		
3760.0	25.2	8		4530.5	32.9		
3913.7	21.2	9		4613.2	13.9		
3947.2	20.9	10		4727.3			
4005.3	11.3						
4025.2	8.3						
4068.0	12.6						
4130.7	11.2						
4201.8	13.8						
4218.1	8.5						
4228.4	12.7						
4261.0	8.4						
4271.3	14.4						
4300.1	11.3						
4330.9	29.9	11					
4365.5	14.7						
4399.9	9.0						
4410.7	14.8	12					
4451.9	32.8						
4552.6	21.8	13					
4646.6	17.0						
4712.8	29.3	14					
4744.6							

TABLE B-1

CAVERN 111

SHEET 1 OF 2

HOLE A				HOLE B			
DEPTH TO TOP OF ANHYDRITE	THICKNESS FT.	CORRELATION		DEPTH TO TOP OF ANHYDRITE	THICKNESS FT.	CORRELATION	
		CAVERN	SITE			CAVERN	SITE
2164.4	7.2	1		2133.6	18.5		
2173.0	6.3	2		2155.2	30.1		
2181.5	7.3	3		2227.3	7.2		
2198.4	6.8	4		2266.8	12.0		
2249.6	7.0	5		2303.2	9.0		
2268.2	10.6			2513.7	11.2	4	
2283.2	9.5			2576.1	11.2	5	
2296.9	11.9	6	H	2596.4	9.3		
2311.6	7.5			2610.3	20.7	6	
2343.3	8.8			2703.8	5.9		
2354.5	6.6			2715.9	20.4		
2393.5	12.4			2766.9	7.9	7	
2452.0	9.5	7		2777.0	6.3		
2464.9	5.1			2791.3	14.9		
2479.2	11.7			2815.9	11.2	8	
2499.4	9.9	8		2841.5	20.3		
2517.9	8.7			2866.4	6.2		
2529.1	7.1			2886.4	9.3		
2560.7	11.3			2912.2	10.7	9	
2588.4	6.2			2973.3	15.4		
2597.0	8.3	9		3038.2	17.7	10	
2615.4	16.4			3070.1	11.6	11	
2733.0	7.4			3090.2	9.8	12	
2741.7	6.5			3133.0	13.0		
2754.0	15.7	10		3163.8	9.5		
2791.2	8.4	11		3186.8	14.8	13	
2814.8	9.8	12		3216.7	14.6	14	
2851.3	11.5			3242.0	14.6	15	
2876.1	6.5			3369.2	9.2	16	
2905.4	19.8			3380.3	8.3		
2948.3	11.3	13		3407.5	21.3	17	
2975.0	14.1	14		3446.6	6.1		
2994.9	8.9			3454.8	15.4	18	
3011.7	8.2	15		3541.7	12.3		
3024.0	5.5			3566.4	12.6		
3138.4	10.7	16		3650.9	10.1		

TABLE B-1

HOLE A			HOLE B		
DEPTH TO TOP OF ANHYDRITE	THICKNESS FT.	CORRELATION CAVERN SITE	DEPTH TO TOP OF ANHYDRITE	THICKNESS FT.	CORRELATION CAVERN SITE
3191.5	17.8	17	3716.4	0.2	
3249.7	45.4	18	3718.1	8.7	
3400.8	12.5		3840.7	22.0	19
3427.6	10.5		3873.5	10.9	
3453.6	24.4		3889.8	13.2	
3659.0	10.1	19	3905.3	9.6	20
3709.4	9.8		3944.0	32.4	21
3731.1	38.2	20	4047.1	29.3	
3786.8	15.9	21	4177.2	13.0	
3812.7	10.4		4260.6	12.2	
4177.6	9.7		4399.8	10.0	
4195.0	13.0		4510.6	30.7	
4295.4	9.3		4572.4	10.7	
4336.3	7.1		4659.6	17.6	
4351.1	15.8		4709.1	7.8	
4379.3	4.2		4722.3	13.0	
4422.6	22.1		4762.9	9.4	
4461.0	10.1		4774.5		
4497.8	9.2				
4515.6	8.3				
4542.3	13.2				
4566.6	16.1				
4637.3	11.2	22			
4681.5	10.7				
4724.9	9.9				
4738.8	9.1				
4788.8	16.3				
4824.2	15.0				
5082.8	6.1				
5092.5	5.8				
5099.6	23.8	23			
5125.2	8.9				
5195.9	13.8				
5221.4	12.7	24			
5355.1	12.0				
5371.4	13.5	25			
5393.8	10.8				
5452.5					

TABLE B-1

CAVERN 112							
HOLE A				HOLE B			
DEPTH TO TOP OF ANHYDRITE	THICKNESS FT.	CORRELATION		DEPTH TO TOP OF ANHYDRITE	THICKNESS FT.	CORRELATION	
		CAVERN	SITE			CAVERN	SITE
2340.9	16.8			2249.1	11.8		
2362.4	14.1			2351.5	10.2		
2378.2	13.4	1	M	2402.6	12.0	0	P
2394.2	14.3			2600.5	21.5	1	
2537.8	9.4			2623.5	13.4		
2595.0	10.4			2711.4	8.4		
2609.5	15.2	2	I	2775.7	13.8		
2642.2	18.5			2833.8	14.9		
2708.8	20.2			2912.2	20.5	2	K
2824.8	11.2			2986.3	10.5		
2846.7	9.3			3030.4	10.7	3	L
2983.2	12.8	6		3089.0	15.8		
3006.6	8.6			3164.8	15.5	4	
3067.1	27.6			3198.1	8.5		
3533.8	9.5			3255.5	16.3		
3557.5	10.4			3305.1	11.5		
3590.6	10.0	7		3325.2	10.5	6	
3613.6	5.2			3397.9	15.1		
3625.0	7.3			3433.7	9.7		
3636.5	7.5			3521.5	12.9		
3659.0	7.4			3634.6	12.7		
3669.3	10.1			3759.7	23.7		
3682.1	18.6			3864.3	21.8	7	
3735.9	10.9			3946.6	10.8		
3757.9	9.6			4095.9	14.1		
3801.1	18.2			4146.4	8.0		
3946.8	20.4			4262.9	28.3		
3992.5	42.5	8		4305.4	14.0	8	
4113.6	13.8	9		4337.5	12.0		
4129.3	6.5			4427.8	7.7	9	
4138.6	8.0			4447.1	9.4		
4223.2	33.7	10	Q	4564.4	5.6		
4479.7	18.8			4581.4	4.3		
4644.3	18.2			4589.4	8.2	10	
4714.7	10.3			4662.3	29.9		
4760.9				4708.1	9.2		
				4762.2			

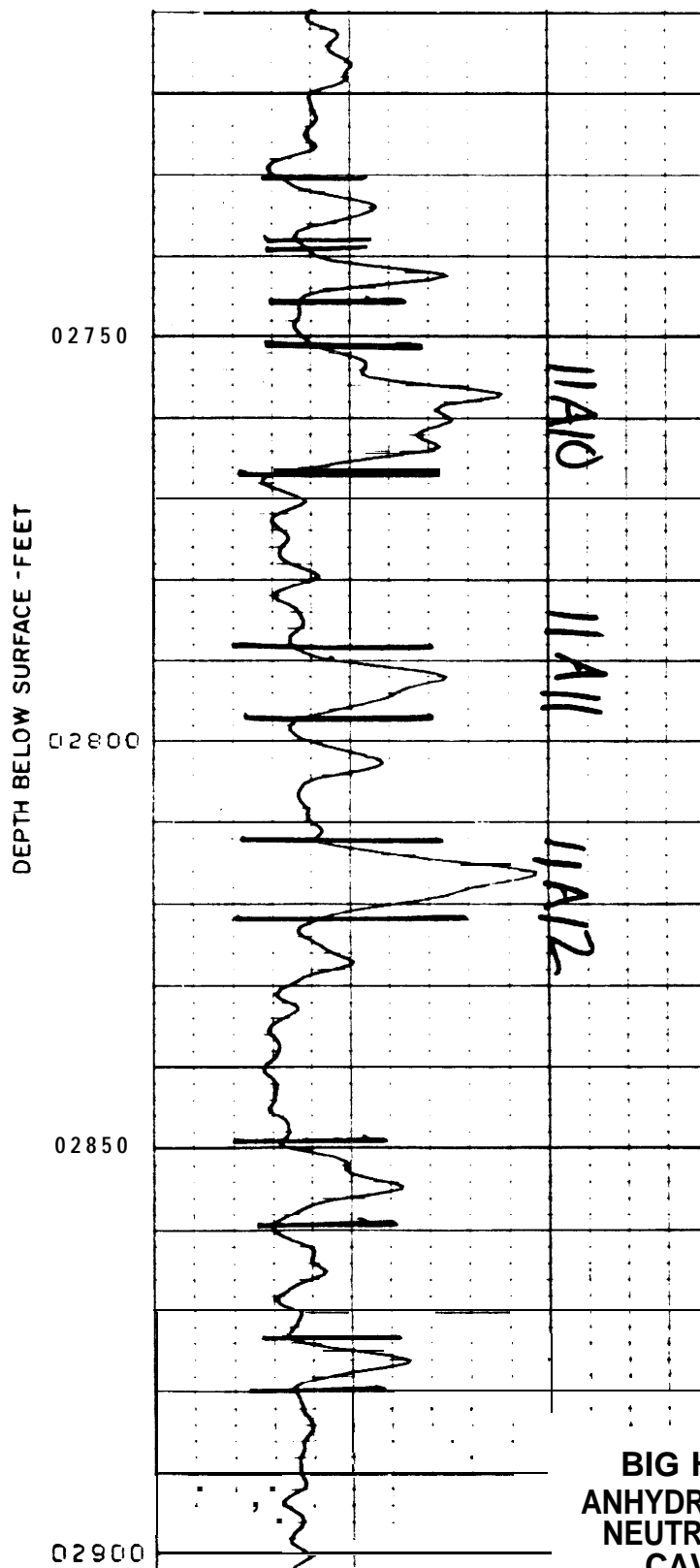
TABLE B-1

CAVERN 113							
HOLE A				HOLE B			
DEPTH TO TOP OF ANHYDRITE	THICKNESS FT.	CORRELATION		DEPTH TO TOP OF ANHYDRITE	THICKNESS FT.	CORRELATION	
		CAVERN	SITE			CAVERN	SITE
2362.3	12.6			2161.0	16.5		
2428.7	12.3			2374.3	26.6		
2585.7	10.0			2403.1	17.2		
2617.1	11.1			2442.8	20.3		
2633.8	10.4			2466.5	31.2		
2774.9	9.8			2532.7	15.8		
2796.9	15.6			2563.9	17.3		
2900.0	13.6			2643.6	23.8	0	I
2961.6	9.8			2754.2	27.3		
3010.2	25.9			2799.6	12.8		
3108.5	8.6			3236.2	14.5		
3686.1	21.3			3263.9	11.4		
3762.6	21.7			3288.6	26.7		
3790.9	11.9			3334.5	13.2		
3856.6	12.0			3384.8	12.5	2	
3887.3	13.2	1		3411.3	25.6	3	M
3972.6	8.2	2		3460.9	9.4		
4005.5	8.3	3		3476.5	8.2		
4085.4	6.6			3489.4	5.8		
4226.4	16.5			3568.9	14.5		
4329.6	10.7			3691.0	21.9		
4375.3	21.1			4000.2	27.3		
4421.2	18.7			4070.6	21.9		
4457.5	17.4			4132.3	23.8		
4484.2	18.2			4188.1	22.5		
4536.5	11.1			4236.1	21.9		
4751.1				4309.6	11.6		
				4538.7	34.9		
				4599.1	18.8		
				4734.0			

TABLE B-1

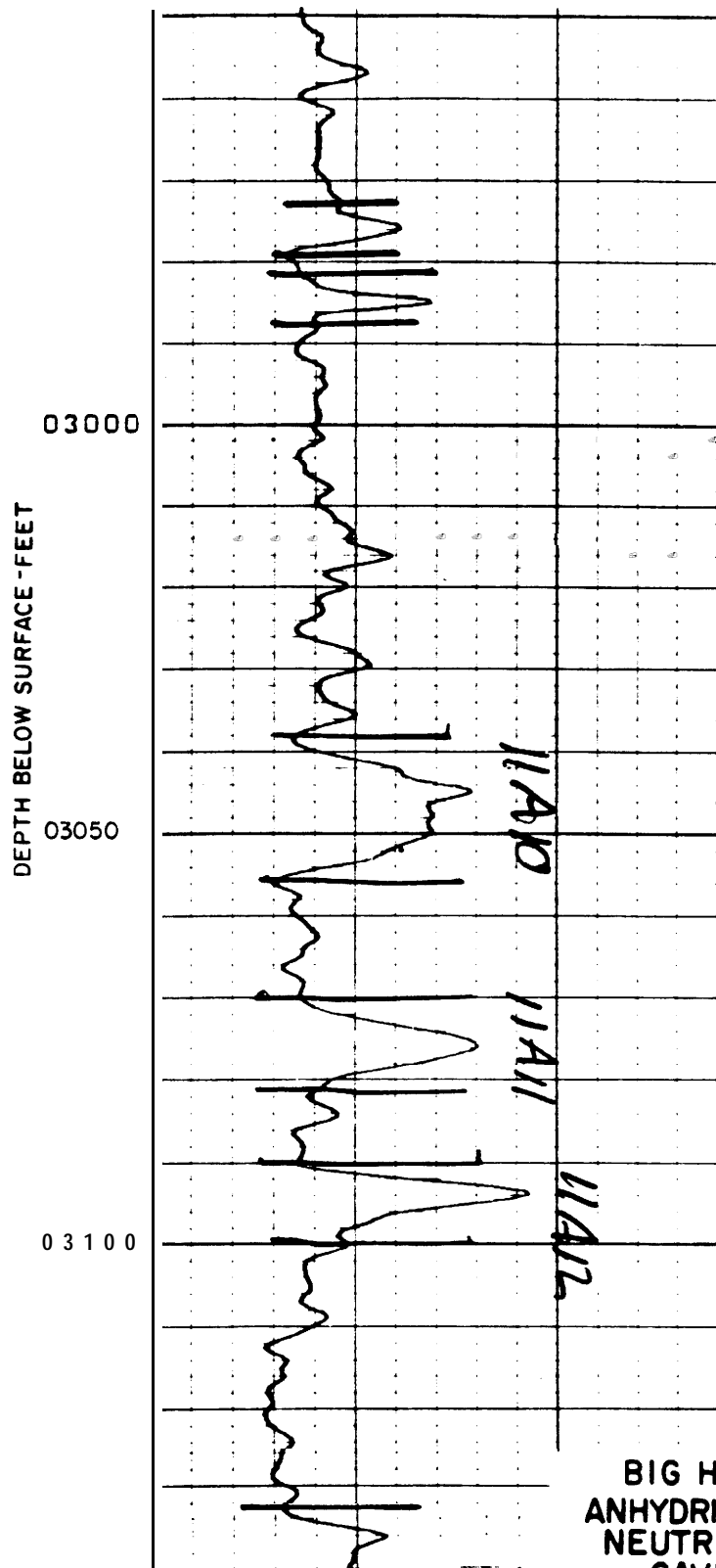
CAVERN 114							
HOLE A				HOLE B			
DEPTH TO TOP OF ANHYDRITE	THICKNESS FT.	CORRELATION		DEPTH TO TOP OF ANHYDRITE	THICKNESS FT.	CORRELATION	
		CAVERN	SITE			CAVERN	SITE
2212.9	63.5			2256.4	18.8		
2496.2	38.1			2277.2	27.7		
2663.6	13.1			2374.8	16.1		
2898.7	12.0			2535.2	14.1		
2947.8	10.8			2576.6	23.3		
3113.4	19.5			2651.3	10.3		
3148.3	32.1	1	N	2726.0	9.6		
3197.2	6.1			2769.9	24.8		
3274.6	16.2			2817.0	9.7		
3320.8	15.4			2917.4	43.0		
3357.4	8.3			2970.1	33.6		
3375.7	7.6			3405.1	45.7		
3396.9	6.8			3759.3	16.2		
3536.8	22.4			3812.3	6.1		
3681.2	7.2			3822.0	9.3		
3693.6	7.4			4740.1	18.4		
3753.4	11.6			4798.5	16.9		
3797.4	9.7			4892.9	32.0	2	
3818.8	10.2			5017.5	18.5		
3933.3	24.9			5069.5	11.1		
4105.0	17.5			5152.0	12.6		
4143.3	13.2			5422.7			
4162.5	18.6						
4217.7	15.4						
4318.7	15.9						
4389.0	8.4						
4441.8	28.7						
4541.1	27.8	2					
4596.5	18.0						
4644.9	22.3						
4675.0	22.2						
4724.6							

TABLE B-1



**BIG HILL SALT DOME
ANHYDRITE CORRELATIONS
NEUTRON DENSITY LOG
CAVERN III WELL A**

FIGURE B-1



BIG HILL SALT DOME
ANHYDRITE CORRELATIONS
NEUTRON DENSITY LOG
CAVERN III WELL B

FIGURE B-1

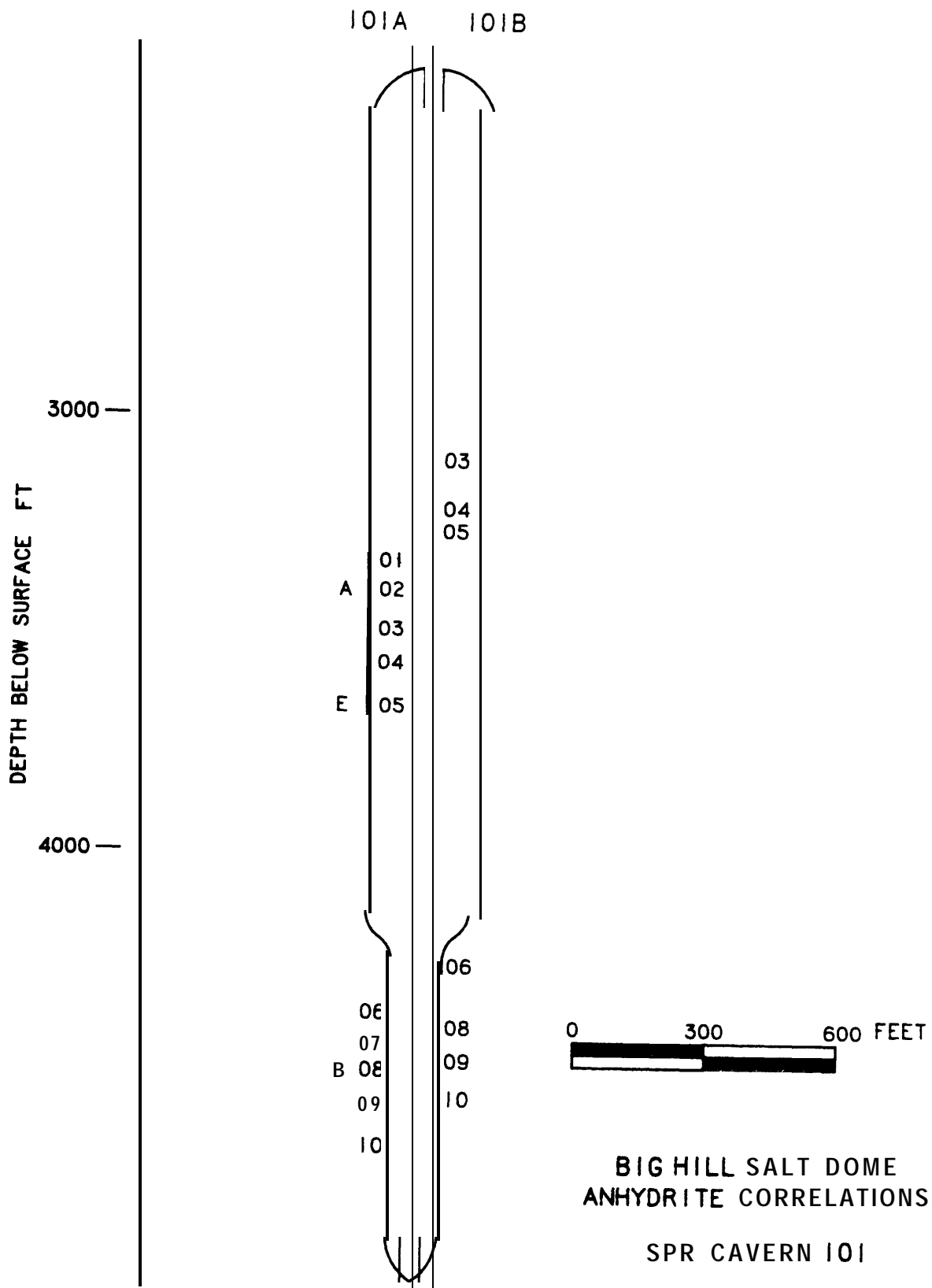
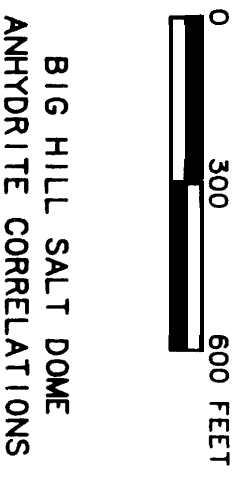
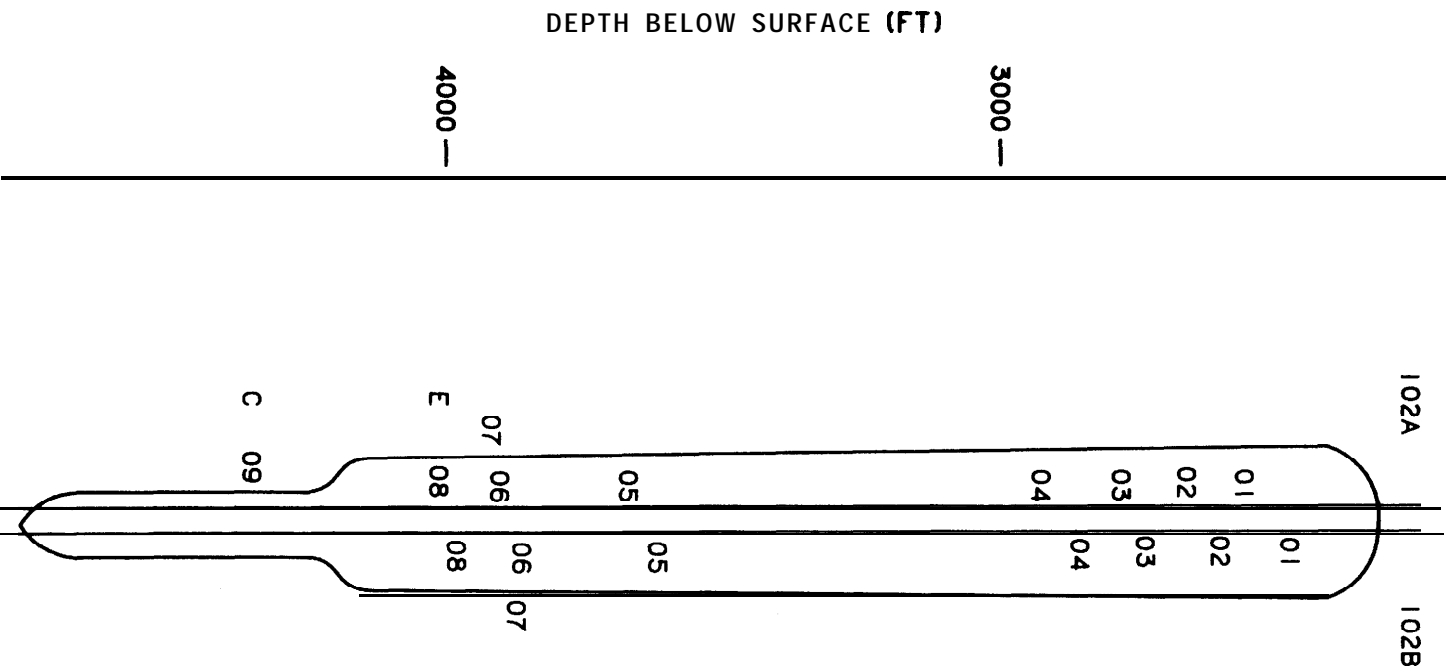


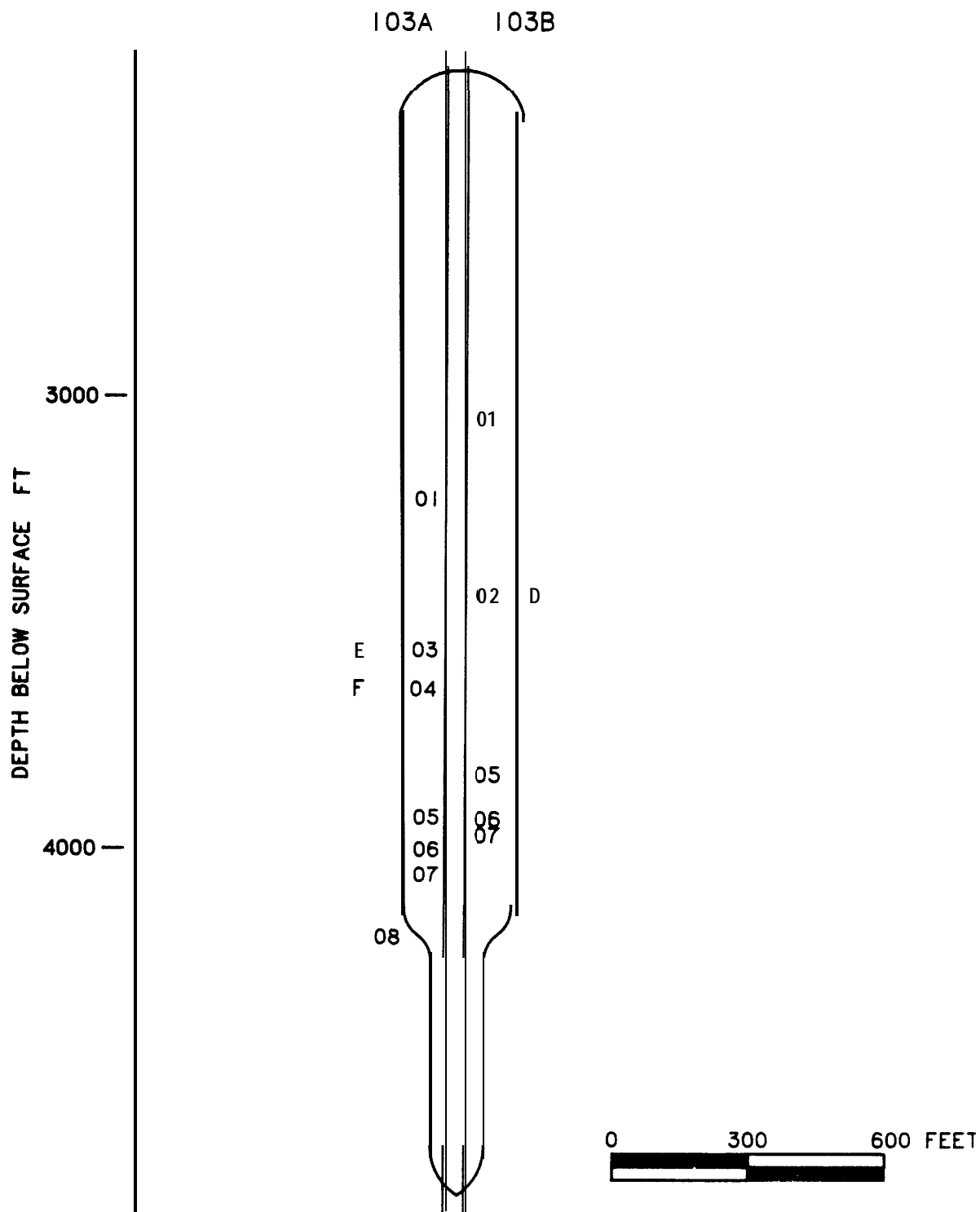
FIGURE B-2



BIG HILL SALT DOME
ANHYDRITE CORRELATIONS

SPR CAVERN 102

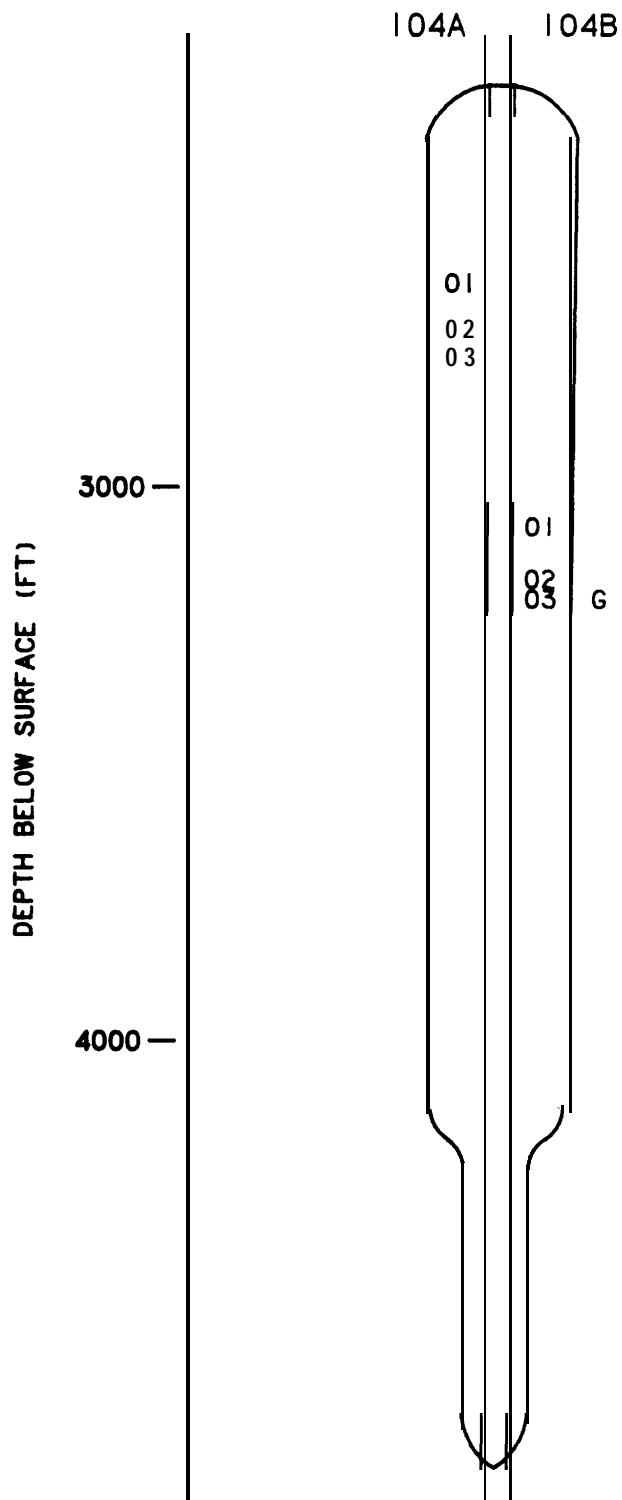
FIGURE B-2



BIG HILL SALT DOME
ANHYDRITE CORRELATIONS

SPR CAVERN 103

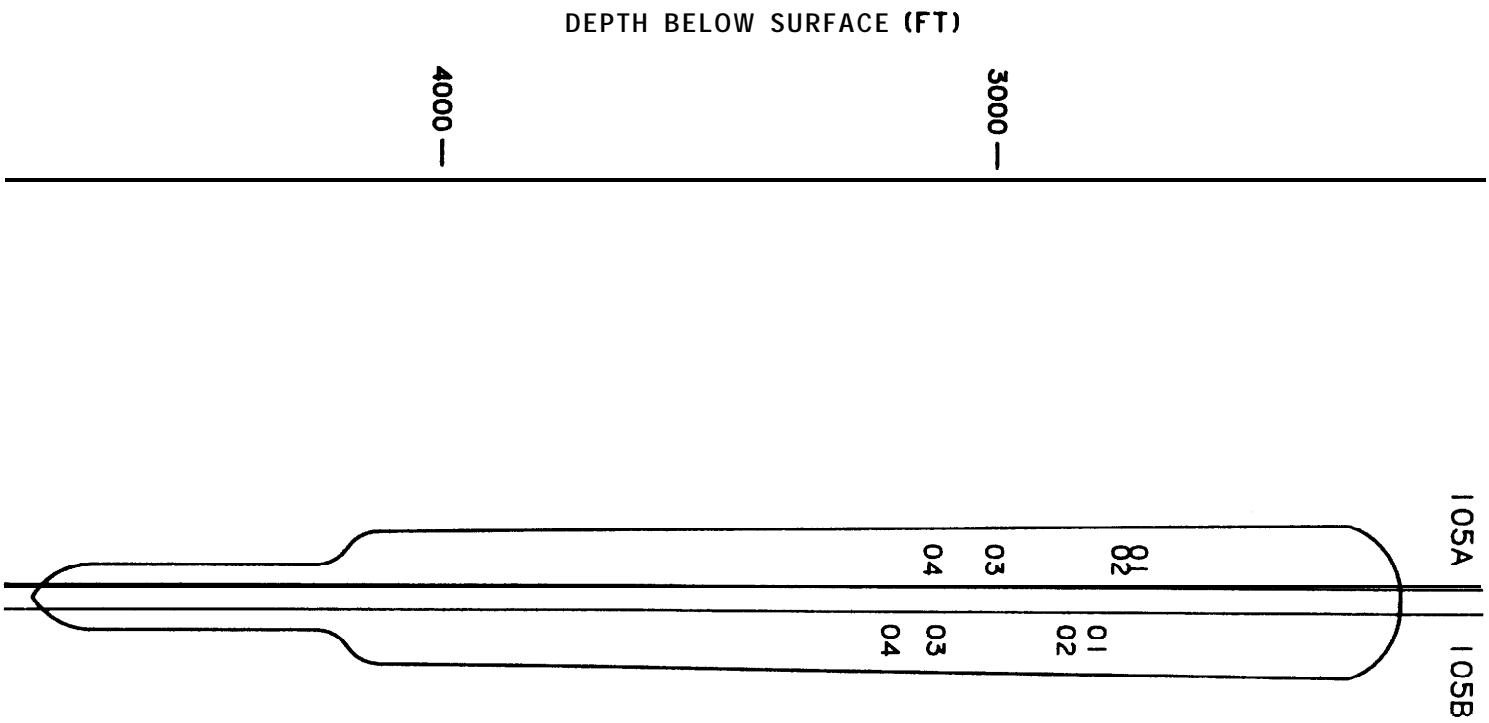
FIGURE B-2



BIG HILL SALT DOME
ANHYDRITE CORRELATIONS

SPR CAVERN 104

FIGURE B-2



BIG HILL SALT DOME
ANHYDRITE CORRELATIONS

SPR CAVERN 105

FIGURE B-2

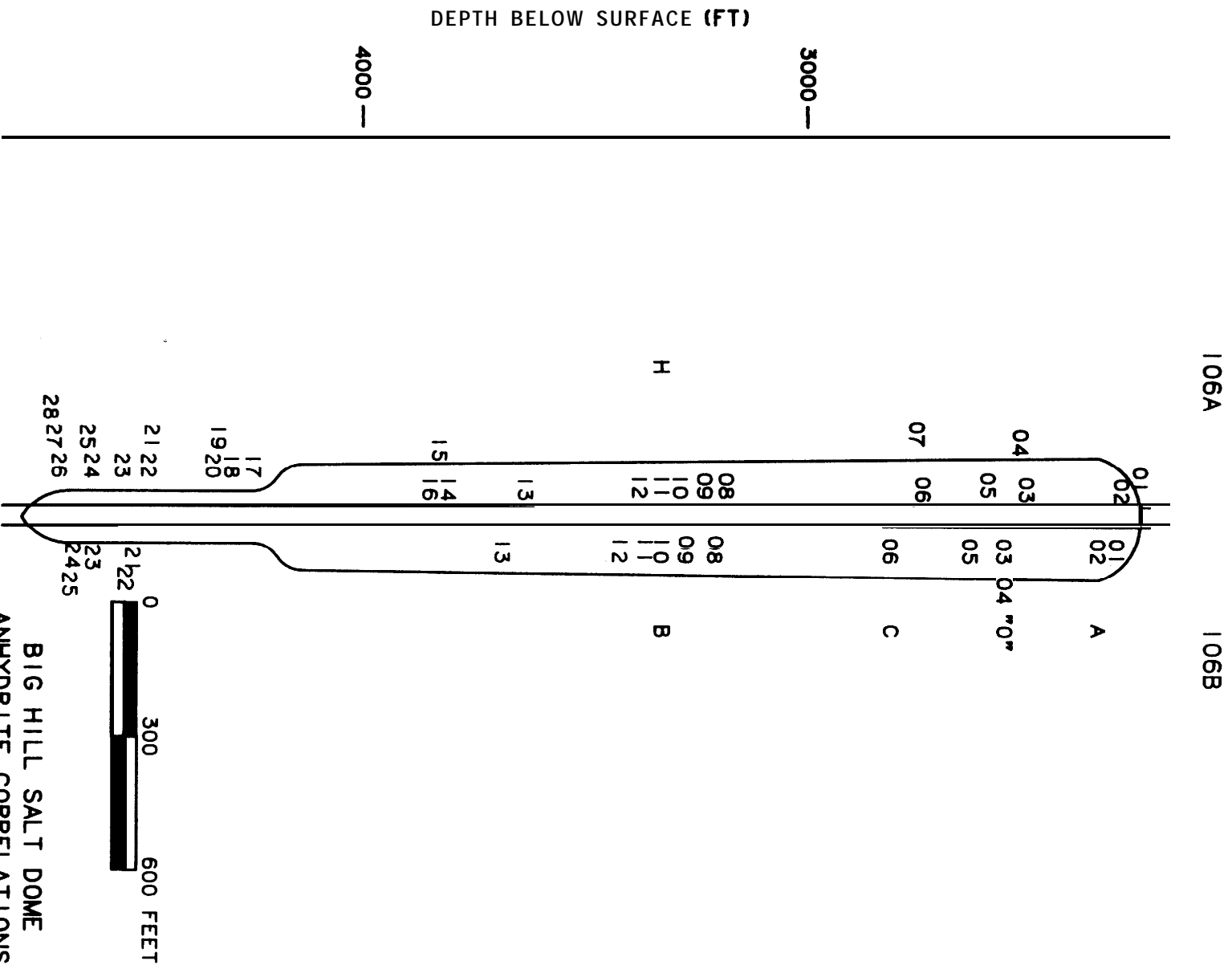
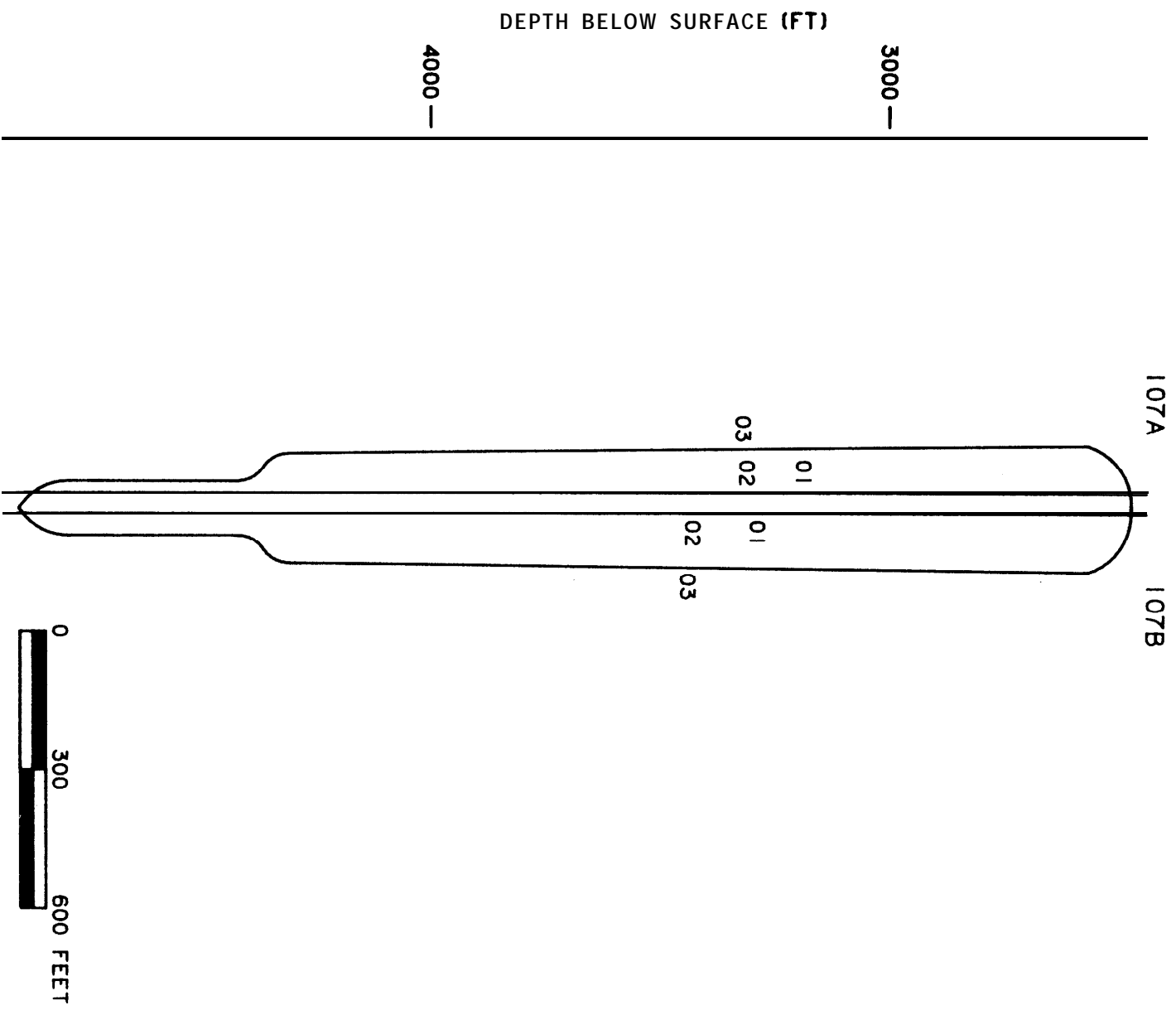
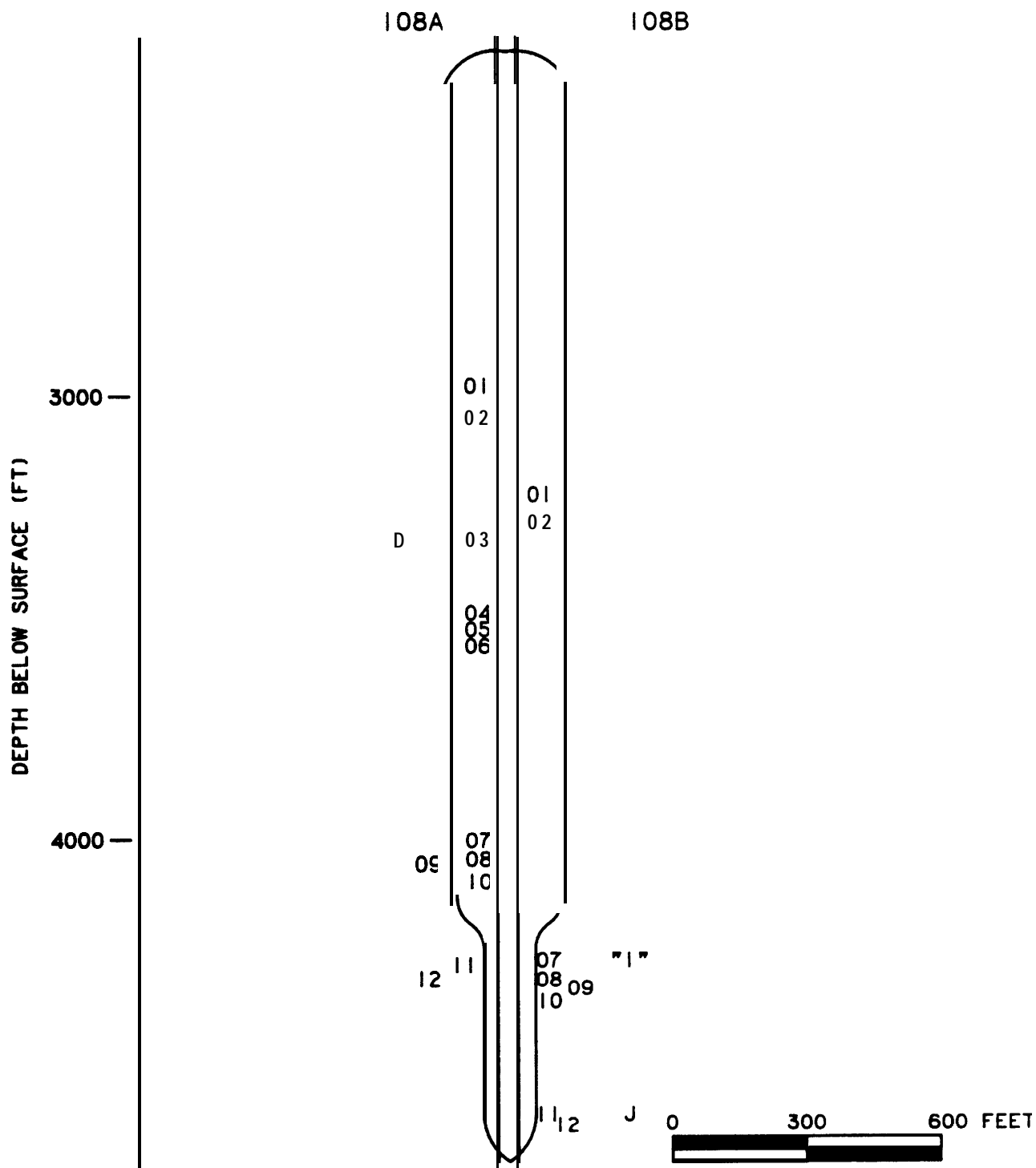


FIGURE B-2



BIG HILL SALT DOME
ANHYDRITE CORRELATIONS
SPR CAVERN 107

FIGURE B-2



BIG HILL SALT DOME
ANHYDRITE CORRELATIONS

SPR CAVERN 108

FIGURE B-2

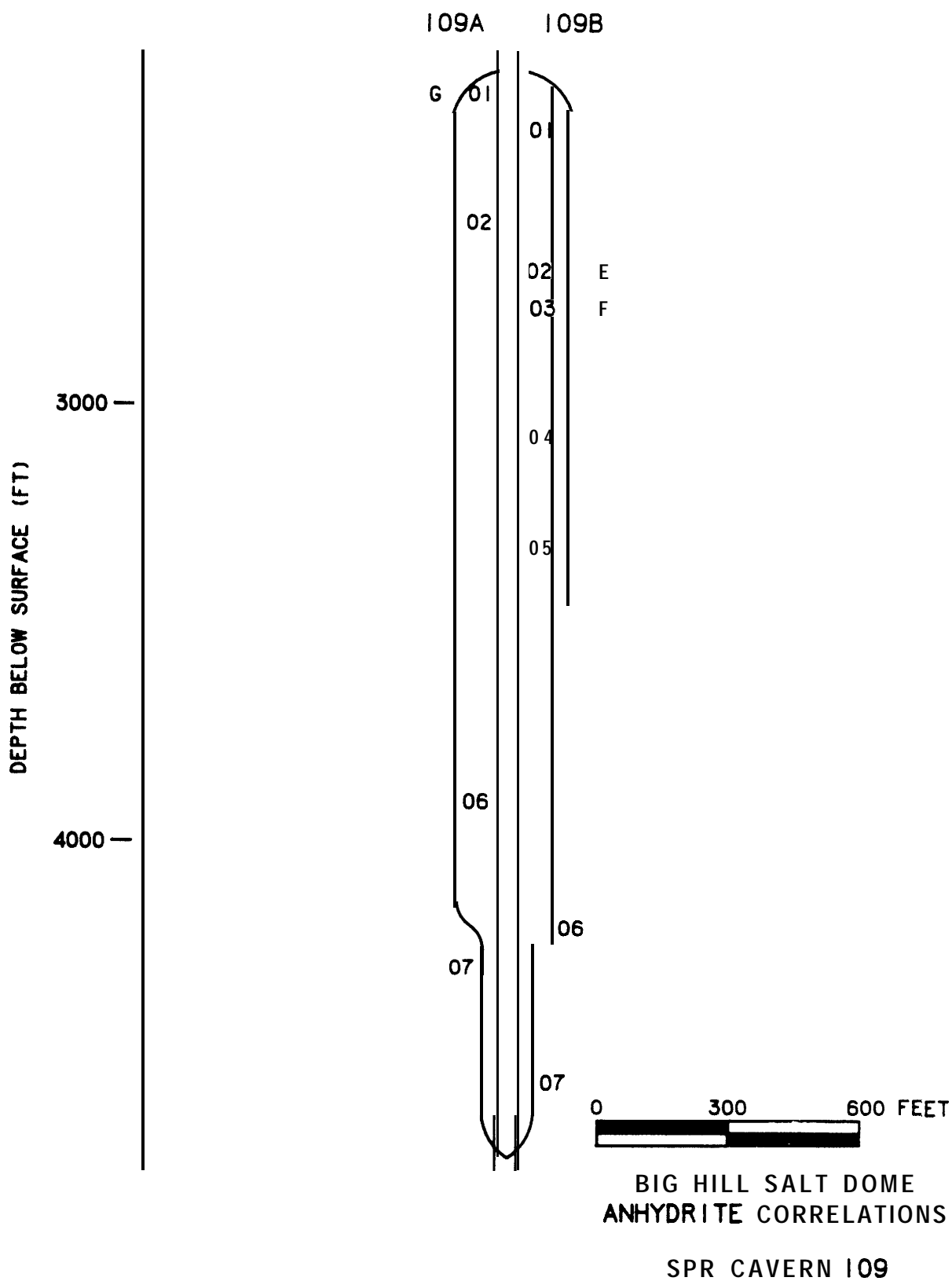


FIGURE B-2

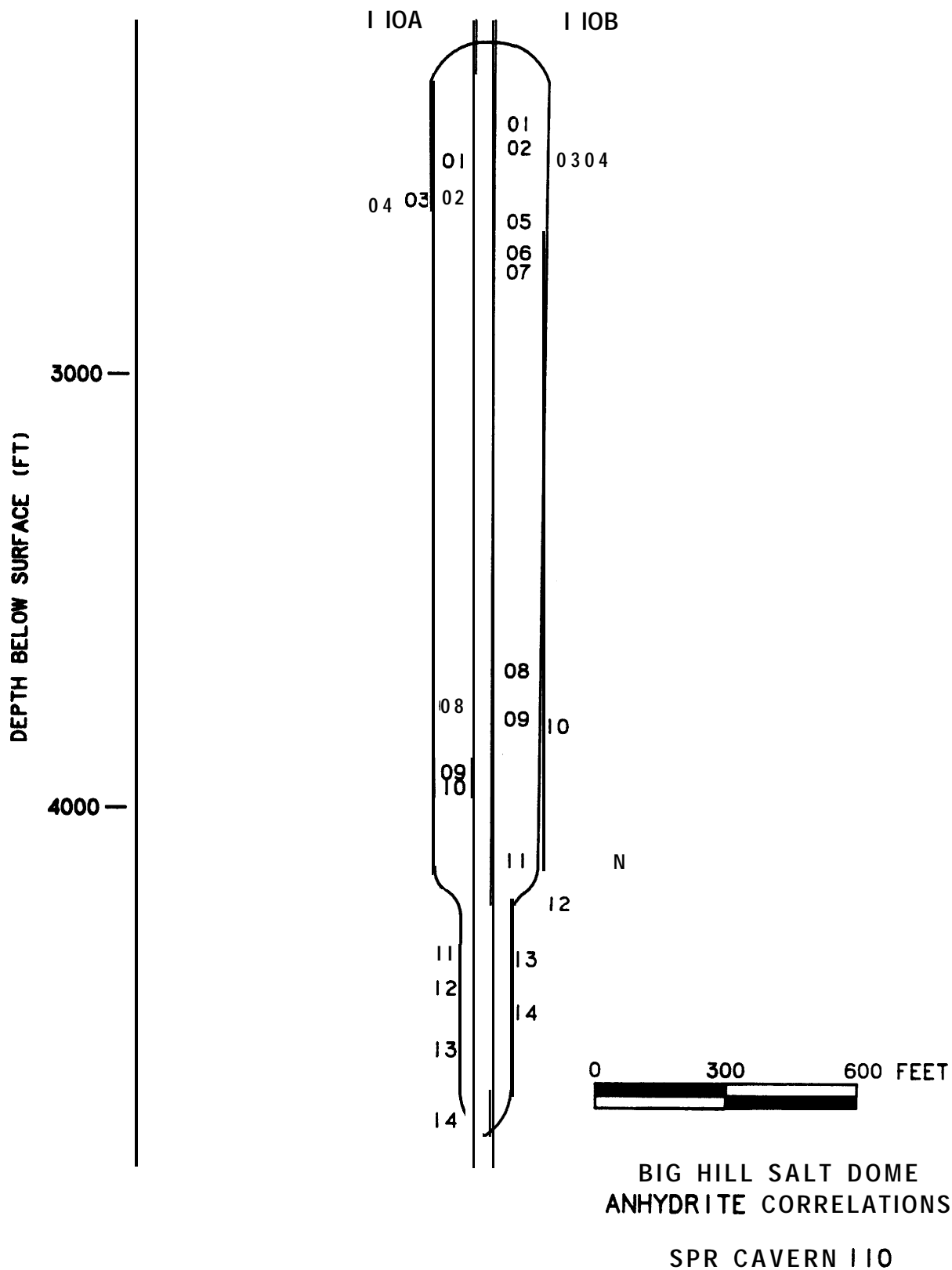
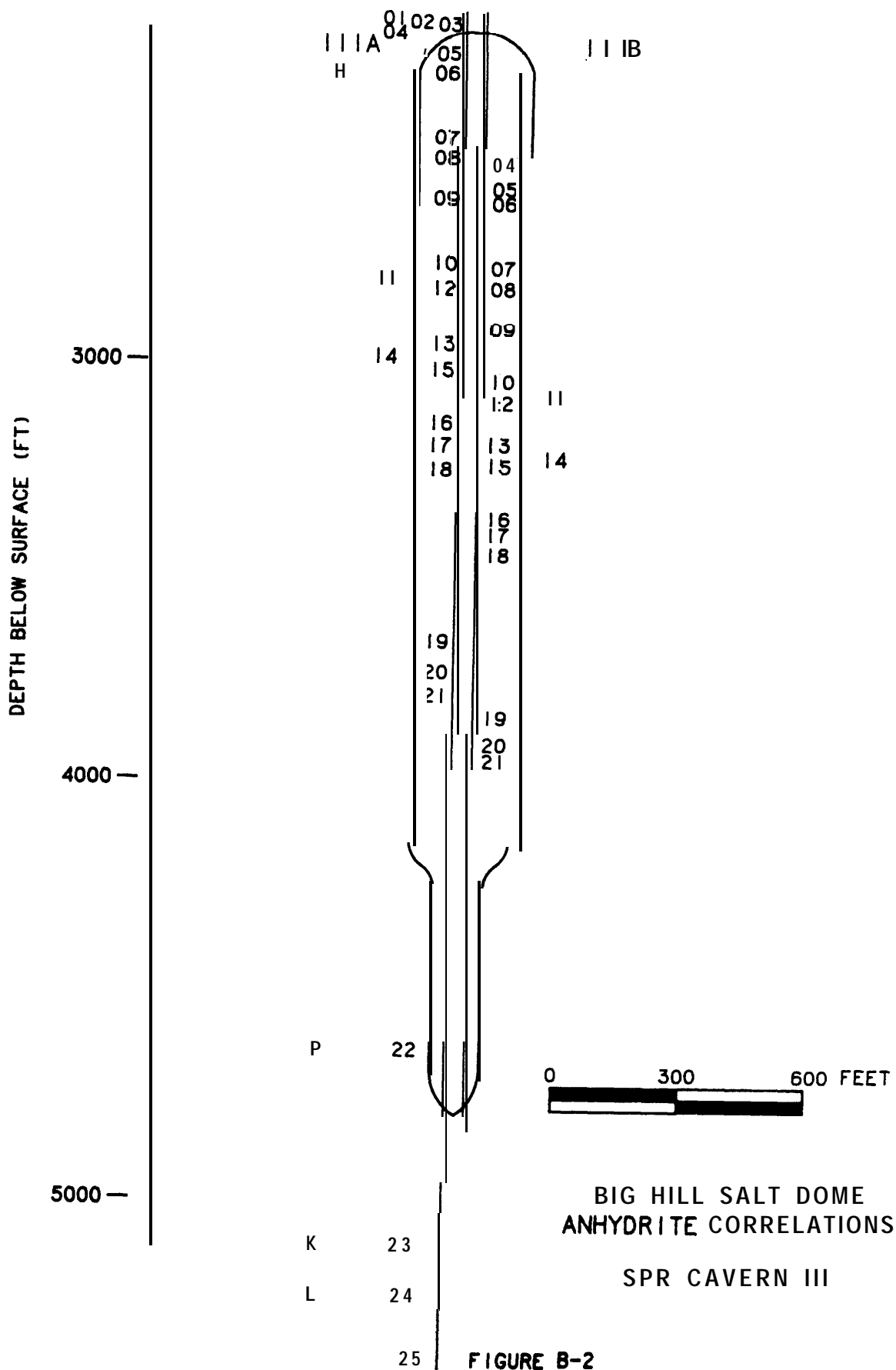
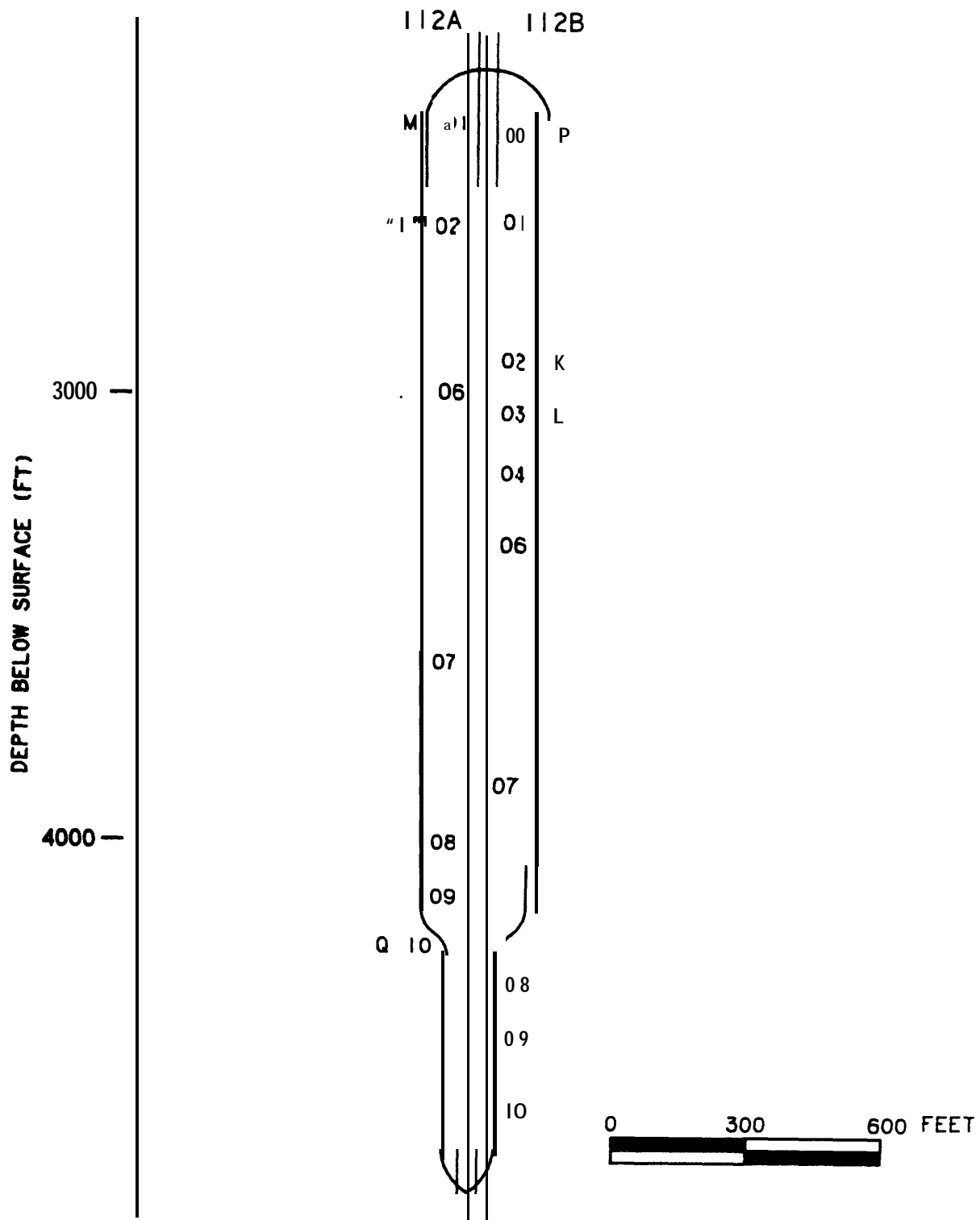


FIGURE B-2

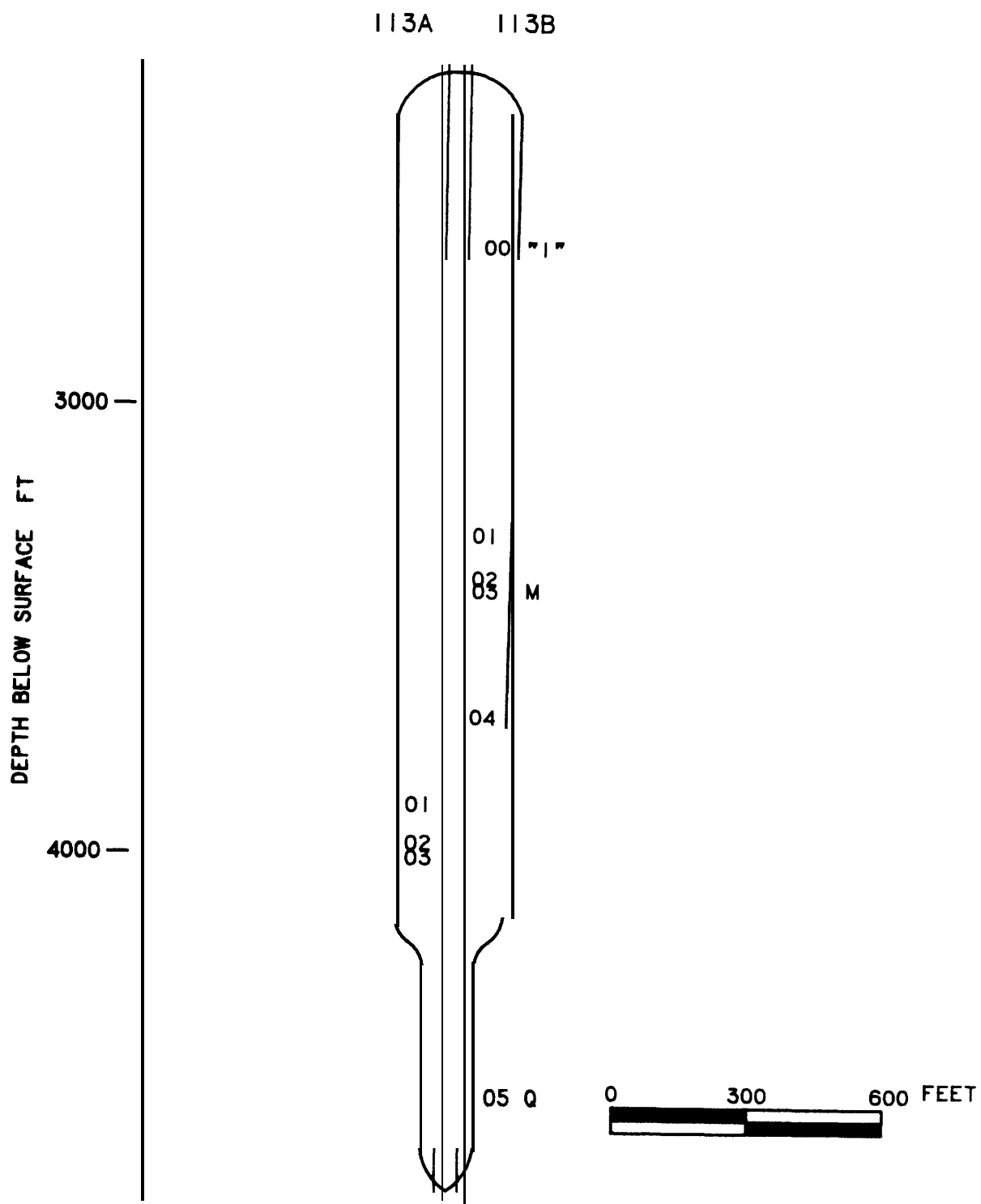




**BIG HILL SALT DOME
ANHYDRITE CORRELATIONS**

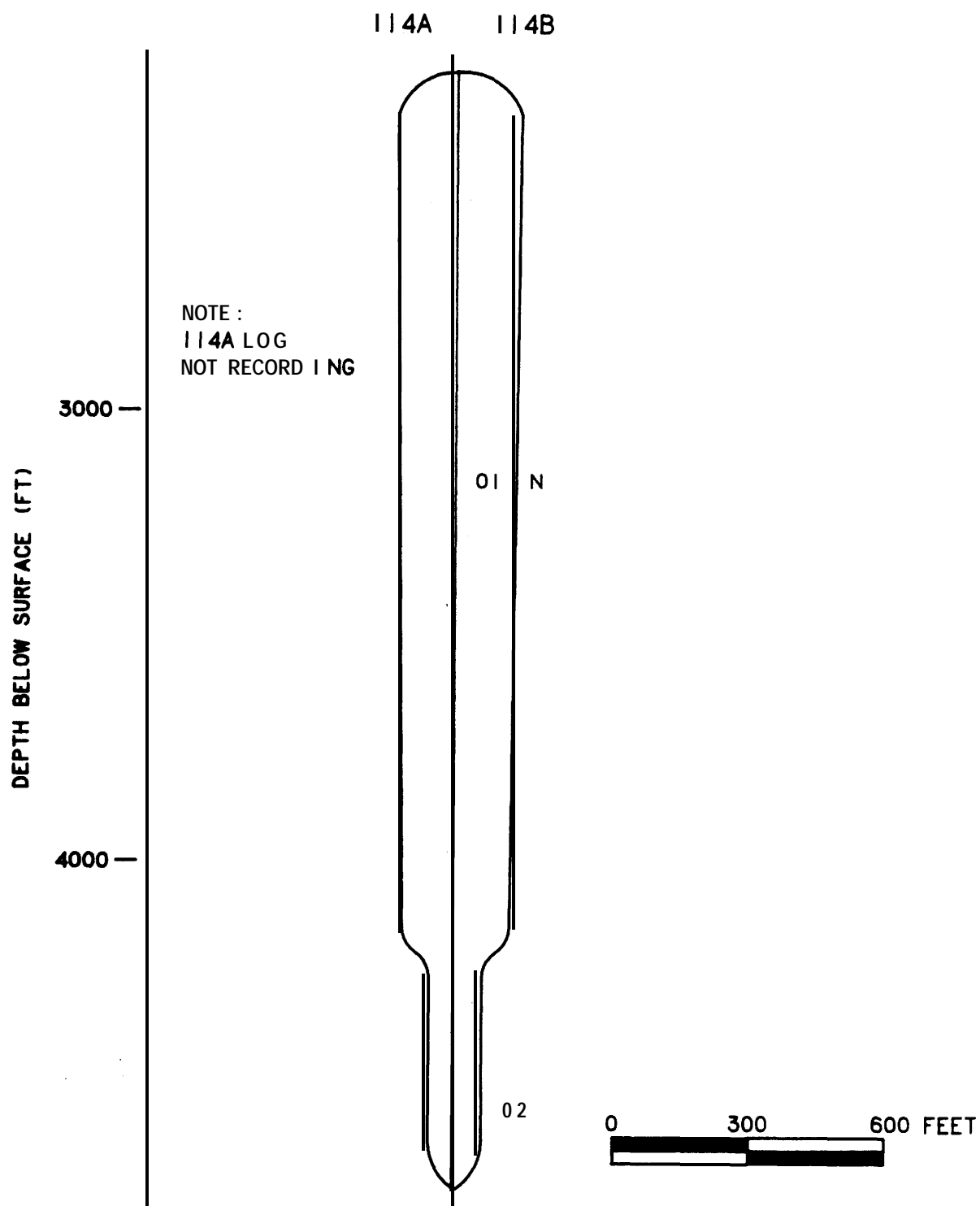
SPR CAVERN 112

FIGURE B-2



BIG HILL SALT DOME
 ANHYDRITE CORRELATIONS
 SPR CAVERN 113

FIGURE B-2



BIG HILL SALT DOME
ANHYDRITE CORRELATIONS

SPR CAVERN 114

FIGURE B-2

ANHYDRITE			
CAVERN	HOLE A %	HOLE B %	AVERAGE %
101	1.1	1.4	1.3
102	1.7	1.6	1.7
103	1.0	1.1	1.1
104	1.6	1.8	1.7
105	2.4	1.0	1.7
106	2.5	2.3	2.4
107	0.7	0.5	0.6
108	1.4	1.7	1.5
109	2.1	1.9	2.0
110	3.2	2.1	2.7
111	2.3	2.4	2.4
112	1.7	1.7	1.7
113	1.2	1.9	1.6
114	1.9	1.2	1.5
AVERAGE =			1.7 %

TABLE B-2

REFERENCES

- Balk, R., 1949, Structure of the Grand Saline Salt Dome, Van Zandt County, Texas: American Association Petroleum Geological Bulletin, v. 33, pp. 1791-1829.
- Balk, R., 1953, Salt Structure of Jefferson Island Salt Dome, Iberia and Vermilion Parishes, Louisiana: American Association Petroleum Geology Bulletin, v. 37, pp. 2455-2474.
- Dobbin, C. E., 1935, Geology of Natural Gas, Am. Assoc. of Pet. Geol. **Bull.** p. 1069. Revised as Natural Gases of North America, v.2, 1968, p. 1966.
- Goin, K. L. and J. T. Neal, 1988, Analysis of Surface Subsidence of the Strategic Petroleum Reserve Crude Oil Storage Sites from December 1982 to January 1988. Sandia National Laboratories, New Mexico, Report **SAND88-1309**, June 1988.
- Halbouty, M. T., 1979, Salt Domes: Gulf Region, United States and Mexico, 2nd Edition, Gulf Publishing Co., Houston, TX.
- Hanna, M. A., 1926, Gulf Coast Salt Domes, In Salt Domes, Am. Assoc. Pet. Geol., Tulsa.
- Humphris, C. C., Jr., 1978, Salt Movements on Continental Slope, Northern Gulf of Mexico; AAPG Studies on Geology 7, pp. 69-85.
- Myers, J. C., 1968, Natural Gases of North America, V. 2, p. 1950. Sulfur - Its Occurrence. Figure 1. Sulfur-bearing domes, Gulf Coast Regions.
- Kupfer, D. H., 1962, Structure of Morton Salt Company Mine, Weeks Island Salt Dome, Louisiana: AAPG Bulletin, v. 46, pp. 1460-1467.
- Kupfer, D. H., 1974, Boundary Shear Zones in Salt Stocks, in A. H. Coogan, ed., 4th Symposium on Salt: Northern Ohio Geological Society, v. 1, pp. 215-225.
- Neal, J. T., 1988, Subsidence Monitoring and Evaluation Plan for Strategic Petroleum Reserve Storage Sites, Sandia National Laboratories, Albuquerque, NM, **SAND88-1175**, September 1988.
- Levorson, A. I., 1954, Geology of Petroleum, Freeman and Company, San Francisco, p. 367.
- SAND81-1045**, Strategic Petroleum Reserve (SPR) Geological Site Characterization Report: Big Hill Salt Dome. Sandia National Laboratories, Albuquerque, NM, September 1981.

Talbot, C. J. and M. P. A. Jackson, 1987, Internal Kinematics of Salt
Diapirs. Am. Assoc. Pet. Geol. Bull., **v.** 71, No. 9, p. 1068-93.

University of Tulsa, 1985, Letter Report, W. Moran to R. R. Beasley, Sandia
National Laboratories, Division 6257 Files.

Distribution:

U.S. DOE SPR PMO (9)
900 Commerce Road East
New Orleans, LA 70123
ATTN: D. R. Spence, PR-62
E. E. Chapple, PR-622
D. W. Whittington, PR-622(3)
TDCS (2)
J. Guarisco (2)

U.S. Department of Energy
Strategic Petroleum Reserve
1000 Independence Avenue SW
Washington, D.C. 20585
ATTN: R. Smith

U.S. Department of Energy
Oak Ridge Operations Office
P.O. Box E
Oak Ridge, TN 37831
ATTN: J. Milloway

DOE SPR Big Hill Site (3)
P.O. Box 1270
Winnie, TX 77665
ATTN: A. E. Fruge, DOE
T. G. Hewitt, BPS
B. O'Connell, PB/KBB

Boeing Petroleum Services (3)
850 South Clearview Parkway
New Orleans, LA 70123
ATTN: J. Siemers
T. Eyennann
K. Mills

PB/KBB (2)
850 South Clearview Parkway
New Orleans, LA 70123
ATTN: J. McHenry

Acres International Corporation (2)
140 John James Audubon Parkway
Amherst, NY 70123
ATTN: B. Lamb
S. Thompson

Electric Power Research Institute
3412 Hillview Avenue
P.O. Box 10412
Palo Alto, CA 94303
ATTN: Bhupen (Ben) Mehta

Louisiana Geological Survey
University Station; Box G
Baton Rouge, LA 70893
ATTN: C. G. Groat

Solution Mining Research Institute
812 Muriel Street
Woodstock, IL 60098
ATTN: H. Fiedelman

Texas Bureau of Economic Geology(3)
University Station, Box X
Austin, TX 78713
ATTN: W. L. Fisher
M. P. A. Jackson
S. J. Seni

Joseph D. Martinez
3641 S. Lakeshore Drive
Baton Rouge, LA 70808

Salt Mining and Technical Storage
Center
Dow Chemical Company
Bldg. S-201
Freeport, TX 77541
ATTN: Ralph Watts, Tech. Mgr.

T. R. Magorian (12)
133 South Drive
Amherst, NY 14226

Union Oil Company
P.O. Box 237
Nederland, TX 77627
ATTN: R. Thompson

Amoco Production Co.
P.O. Box 3092
Houston, TX 77001
ATTN: E. Steffens

T. S. Ortiz
20 Riverside Road
Los Lunas, NM 87031

R. Ginn
Underground Injection Control
Railroad Commission of Texas
Austin, TX 78711-2967

1521	R. D. Krieg
1521	H. S. Morgan
1521	D. J. Segalman
3141	S. A. Landenberger (3)
3154-1	C. Ward, for: DOE/OSTI(8)
3151	W. I. Klein (3)
6000	D. L. Hartley
6200	V. L. Dugan
6225	H. J. Sutherland
6230	W. C. Luth
6231	H. C. Hardee
6231	W. R. Wawersik
6232	D. H. Zeuch
6250	R. K. Traeger
6253	J. C. Lorenz
6257	J. K. Linn (10)
6257	J. L. Todd
6257	J. T. Neal (15)
6258	D. S. Preece
6332	L. D. Tyler
8524	J. R. Wackerly